

UNCLASSIFIED

AD 288 118

*Reproduced
by the*

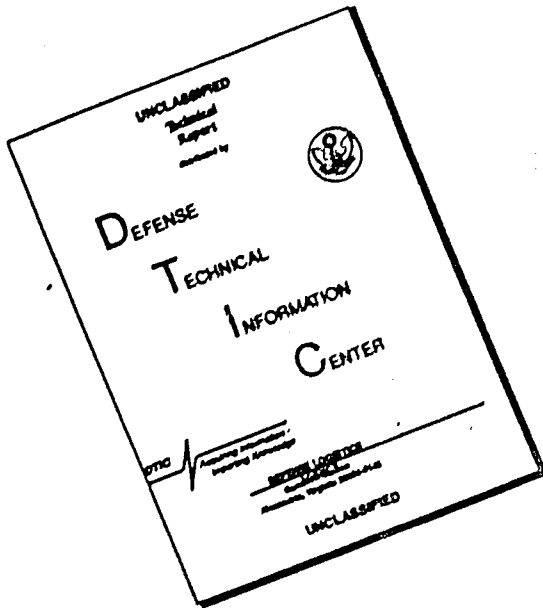
ARMED SERVICES TECHNICAL INFORMATION AGENCY
ARLINGTON HALL STATION
ARLINGTON 12, VIRGINIA



UNCLASSIFIED

NOTICE: When government or other drawings, specifications or other data are used for any purpose other than in connection with a definitely related government procurement operation, the U. S. Government thereby incurs no responsibility, nor any obligation whatsoever; and the fact that the Government may have formulated, furnished, or in any way supplied the said drawings, specifications, or other data is not to be regarded by implication or otherwise as in any manner licensing the holder or any other person or corporation, or conveying any rights or permission to manufacture, use or sell any patented invention that may in any way be related thereto.

DISCLAIMER NOTICE



THIS DOCUMENT IS BEST
QUALITY AVAILABLE. THE COPY
FURNISHED TO DTIC CONTAINED
A SIGNIFICANT NUMBER OF
PAGES WHICH DO NOT
REPRODUCE LEGIBLY.

63-1-4

ASTIA

DATA LOG

ACQ. FILE

288118

288118

HYDRONAUTICS, incorporated research in hydrodynamics

Research, consulting, and advanced engineering in the fields of
NAVAL and INDUSTRIAL HYDRODYNAMICS. Offices and Laboratory
in the Washington, D. C., area: 200 Monroe Street, Rockville, Md.

HYDRONAUTICS, Incorporated

TECHNICAL REPORT 117-1

ANALYSIS OF THE BULBOUS BOW
ON SIMPLE SHIPS

by

B. Yim
August 1962

Prepared under
Office of Naval Research
Department of the Navy
Contract Nonr-3349(00)
NR 062-266

HYDRONAUTICS, Incorporated

TABLE OF CONTENTS

	Page No.
LIST OF SYMBOLS	i
LIST OF FIGURES	iii
1. INTRODUCTION	1
2. FORMULATION OF THE BOUNDARY VALUE PROBLEM (CASE I)	3
3. FORCE AT DOUBLET POINT	5
4. NONDIMENSIONAL FORM	7
5. EVALUATION OF INTEGRAL R_o	9
6. FORCE AT SOURCE POINT	12
7. TOTAL FORCE AND OPTIMUM PARAMETERS	13
8. REMARKS	15
9. WAVE HEIGHTS (CASE II)	16
10. HAVELOCK'S FORMULA AND WAVE RESISTANCE	18
11. NONDIMENSIONAL FORM	20
12. OPTIMUM PARAMETERS	21
13. SHIP SHAPES	22
14. DISCUSSION	24
15. WAVE RESISTANCE OF THE SYSTEM OF A DOUBLET LINE AND A SOURCE LINE (CASE III)	25
16. NONDIMENSIONAL FORM	27
17. OPTIMUM PARAMETERS	28
18. EFFECT OF STERN	30
19. DISCUSSION	32
20. APPLICATION	33
APPENDIX	36
REFERENCES	39

HYDRONAUTICS, Incorporated

-i-

LIST OF SYMBOLS

-a	x coordinate of doublet or doublet line
a_i	polynomial coefficients of source distribution
b	radius of a bulb (approximated as a sphere)
d	length of source line
F_f, F_d, F_L	Froude numbers with respect to f, d, and L respectively
f	depth of a point source below the free surface
f_1, f_2	depths of end points of source line
g	acceleration of gravity
$G_n(k_o), I_v$	Integrals defined by Equations [16] and [14] respectively
K_o, K_1	Modified Bessel Functions of the 2nd kind
k_o	$= g/v^2$
L	distance between two vertical source lines fore and aft
m	total strength of a point source or a source line
m_1	$= m/d$
r	radius of half body
R	total wave resistance
R_o, R_s, R_b	
R_{int}, R_{li}, R_{ls}	Parts of Wave resistance defined in Sections 7 and 10.
$R_1(a, b, c), R_2(a, b, c,)$	
Re	= real part of

HYDRONAUTICS, Incorporated

-ii-

$R_i [a k_o, k_o, n]$ an integral defined by Equation [12]

V Uniform free stream velocity at ∞

x, y, z Rectangular right handed coordinate system with origin at free surface, z positive upward, and x in the direction of the uniform flow velocity V

ϕ total velocity potential

$\phi_1, \phi_2, \phi_{10}$ potentials defined in Section 2

μ strength of doublet

μ_1, μ_2 linear coefficients of strength of doublet in $\mu = \mu_1 - z\mu_2$

$v = v_1/V$

v_1 fictitious frictional force

ρ mass density of water

$\omega = (x + a) \cos \sigma + y \sin \sigma$

ζ wave height

ζ_s, ζ_b wave height due to sources and doublets respectively.

HYDRONAUTICS, Incorporated

-iii-

LIST OF FIGURES

FIGURE NO.

1. COORDINATE
2. CONTOUR OF INTEGRATION
3. WAVE RESISTANCE OF HALF BODY WITH OPTIMIZED BULB
4. OPTIMUM DISTANCE BETWEEN SOURCE AND DOUBLET, OPTIMUM RADIUS OF BULB
5. WAVE RESISTANCE OF A SOURCE LINE AND OPTIMUM DOUBLET LINE AT EACH FROUDE NUMBER
6. OPTIMUM DISTANCE BETWEEN DOUBLET AND SOURCE LINE
7. OPTIMUM RADIUS OF BULB (A POINT DOUBLET)
8. OPTIMUM DEPTH OF DOUBLET
9. BODY STREAMLINE SHAPE DUE TO A SOURCE LINE AND A POINT DOUBLET
10. BODY STREAMLINE SHAPE DUE TO A SOURCE LINE AND A POINT DOUBLET
11. BODY STREAMLINE SHAPE OF SOURCE AND SINK LINES AND A POINT DOUBLET
12. OPTIMUM DISTANCE a , BETWEEN DOUBLET LINE AND SOURCE LINE
13. OPTIMUM STRENGTH OF DOUBLET LINE
14. WAVE RESISTANCE OF SOURCE LINE AND DOUBLET LINE (BULB)
15. WAVE RESISTANCE FOR SOURCE LINE SHIP INCLUDING STERN
16. WAVE RESISTANCE INTERFERENCE WITH STERN
17. BODY STREAMLINE SHAPE DUE TO A DOUBLET LINE AND A SOURCE LINE

HYDRONAUTICS, Incorporated

ANALYSIS OF THE BULBOUS BOW ON SIMPLE SHIPS

1. INTRODUCTION

The effect of bulbous bows on the wave resistance of ships was first investigated by the systematic experiments of D. W. Taylor (1911 and 1943), E. M. Bragg (1930), and E. F. Eggart (1935). It had been generally understood that the decrease of resistance due to a bulbous bow is a wave-making phenomenon. J. G. Thews in 1930-1932 conducted experiments to determine the conditions for the cancellation of the bow wave by the bulb. (See H. E. Saunders 1957). In 1928, Havelock calculated the wave form due to a doublet immersed in a uniform stream, and found that a wave trough was formed just aft of the doublet. Since a deeply immersed sphere is equivalent to a doublet, W. C. S. Wigley (1936) investigated this effect with a mathematical model of a Michell's ship plus a doublet. By using Havelock's resistance formula (1934b), he demonstrated the fact that the doublet wave cancels the bow wave and thus lessens the wave resistance. His analytic work was also supplemented and confirmed by his model experiments. G. Weinblum (1935) dealt with this problem by expressing the form of a ship with a bulbous bow in terms of a polynomial according to Michell's thin ship approximation.

Recently Inui, Takahei and Kumano (1960) observed wave profiles and found that the wave due to a ship with a submerged sphere faired into the bow was exactly the superposition of the wave due to the corresponding point doublet and that due to the hull. They explained the effect of the bulb on the wave resistance of a ship by using the idea of Havelock's elementary surface wave (1934a).

The mathematical expression of the wave resistance of a conventional ship is extremely complicated. Except for the special cases of very low or very high Froude numbers it is necessary to integrate a highly oscillating function numerically. And it is extremely difficult to investigate the effect of varying parameters in the wave resistance equation. Therefore, only simple models of ships are considered in the present paper. The advantages of this procedure are: 1) We can analyze not only the wave resistance but also the effect of the size and the location of the bulb. 2) We need not be concerned about the effect of linearizing the boundary condition on the ship surface. 3) We can investigate the fundamental relationship between the source and doublet under the free surface.

At first, the simplest system, a point doublet and a point source, is considered. The so-called interference term of the wave resistance is calculated by a series expansion. The optimum distance between two singularities, and the optimum size and depth of the bulb are obtained. By this procedure we can show that a remarkable reduction in the wave resistance can be realized by the use of bulb.

Second, a system consisting of point doublet and a finite source line is considered. This is treated in similar manner to the first case.

Third, a system consisting of a vertical doublet line under the free surface and a vertical source line from the free surface is considered. The strength of the doublet line is considered to vary linearly. However, the optimum distribution of the strength of the doublet line is found to be almost uniform. The influence of a stern is also considered using the method of stationary phase. In this case, the calculation is performed on

the I.B.M. 1620 Digital Computer.

To obtain the wave resistance, Lagally's theorem is used in the first case while Havelock's formula is used in the second and third cases. When Lagally's theorem is used we can see very clearly how a thrust force is applied at the point of the doublet, when it is located at the proper position in front of the source.

The actual shapes of the low resistance systems are found by computing the actual stream lines. The bulb is found to be very large so that the bulb itself may be considered to be a bow rather than an appendage.

This method of analysis is shown to be applicable to the general case in which the waterline of a ship is expressed as a polynomial.

Case 1

2. FORMULATION OF THE BOUNDARY VALUE PROBLEM

The origin 0 is placed on the mean free surface. The x direction is the same as that of the velocity of the uniform stream. The z axis is directed upward from the surface. The coordinate axes 0-xyz shown in Figure 1 form a right handed system. Symbols are shown in the figures or in the symbol table if not mentioned in the text. The water is, as usual, considered to be incompressible, homogeneous, and inviscid. The motion is considered to be steady.

A system consisting of a doublet at point $(-a, 0, -f)$, a source at point $(0, 0, -f)$ and a sink at point $(L, 0, -f)$ in a uniform stream will represent approximately the combination of a bulb and a Rankine ovoid. The wave resistance due to this system can be obtained by using Lagally's theorem. To investigate mainly the relation between the bulb and bow, we only need consider the

system of the doublet at point $(-a, 0, -f)$ and the source at point $(0, 0, -f)$. We denote ϕ_1 and ϕ_2 as the perturbation potential due to the point doublet and the point source respectively. The symbols m and $-\mu$ denote the strength of the source and the doublet respectively.

Denoting $R(a, b, c)$ as the x component of the force at the point (a, b, c) we obtain by Lagally's theorem (Lagally 1922 or see Milne Thomson 1956).

$$R_1(-a, 0, -f) = -4\pi\rho\mu \frac{\partial}{\partial x} \left[\frac{\partial\phi_{10}}{\partial x} + \frac{\partial\phi_{20}}{\partial x} \right](-a, 0, -f) \quad [1]$$

$$R_2(0, 0, -f) = 4\pi\rho m \left(\frac{\partial\phi_1}{\partial x} + \frac{\partial\phi_{20}}{\partial x} \right) (0, 0, -f) \quad [2]$$

The subscript 0 to ϕ_1 means that we exclude the effect of the point itself.

Now we have only find the perturbed velocities at two points $(-a, 0, -f)$ and $(0, 0, -f)$. The perturbation potential ϕ must satisfy Laplace's equation.

$$\nabla^2 \phi = 0 \quad [3]$$

and the boundary conditions on the free surface and at infinity as well as near the singularities. The linearized kinematic boundary condition on the free surface [see Lamb 1945] is given by

$$\phi_z = -V \zeta_x \quad \text{on } z=0 \quad [4]$$

where ζ is the free surface elevation. If the idea of fictitious frictional force [see Lamb 1945 or Lunde 1952] is used,

HYDRONAUTICS, Incorporated

-5-

the pressure condition on the free surface is

$$\phi_x V - g \zeta + \nu_1 \phi = 0 \quad \text{on } z = 0 \quad [5]$$

ν_1 being the coefficient of the fictitious frictional force.

Combining above the two conditions we obtain

$$\phi_{xx} + k_0 \phi_z + \nu \phi_x = 0 \quad [6]$$

on $z = 0$

where $k_0 \equiv g/V^2$, $\nu \equiv \nu_1/V$.

When the distance from the singularities goes to infinity,

$$\nabla \phi = 0 \quad [7]$$

In addition, we note the empirical fact that the disturbance in front of ship decreases very rapidly when $-x$ becomes large.

3. FORCE AT DOUBLET POINT

The solution of our problem [3] with boundary conditions [6] and [7] can be found in many papers (e.g. Lunde 1952). Using the integral representation

$$\frac{m}{\sqrt{(x+a)^2 + y^2 + (z-f)^2}} = \frac{m}{2\pi} \int_0^{2\pi} d\theta \int_0^{\infty} e^{-k(\sqrt{|z-f|} - i\omega)} dk$$

where $\omega = (x+a) \cos \theta + y \sin \theta$, we have for the potential, due to only the images of the doublet, satisfying the conditions [3], [6] and [7]

$$\phi_{10} = \frac{\mu(x+a)}{\sqrt{(x+a)^2 + y^2 + (z-f)^2}}^{3/2}$$

$$- \operatorname{Re} \frac{k_0}{\pi} \mu \int_{-\pi}^{\pi} \int_0^{\infty} \frac{-i k \sec \theta e^{k(i\omega - |z-f|)}}{k - k_0 \sec^2 \theta - iv \sec \theta} dk d\theta$$

where Re means "real part of". Hence

$$\frac{\partial \phi_{10}}{\partial x} = \mu \left[\frac{1}{\sqrt{(x+a)^2 + y^2 + (z-f)^2}}^{3/2} \right.$$

$$- \frac{3(x+a)^2}{\sqrt{(x+a)^2 + y^2 + (z-f)^2}}^{5/2}$$

$$\left. + \operatorname{Re} \frac{k_0}{\pi} \int_{-\pi}^{\pi} \int_0^{\infty} \frac{k^2 e^{k(i\omega - |z-f|)}}{k - k_0 \sec^2 \theta - iv \sec \theta} dk d\theta \right]$$

The x component of the perturbed velocity due to the source, which satisfies Equations [3], [6] and [7] is

$$\left(\frac{\partial \phi_2}{\partial x} \right)_{x,0,-f} = m \left(-\frac{1}{x^2} + \frac{x}{\sqrt{x^2 + 4f^2}}^{3/2} \right)$$

$$- \operatorname{Re} \frac{k_0 m}{\pi} \int_{-\pi}^{\pi} \int_0^{\infty} \frac{i k \sec \theta e^{k(ix \cos \theta - 2f)}}{k - k_0 \sec^2 \theta - iv \sec \theta} dk d\theta \quad [8]$$

Hence from Equation [1]

$$R_1(-a, 0, -f) = -4\pi\rho\mu \left[\operatorname{Re} \mu \frac{k_o}{\pi} \int_{-\pi}^{\pi} \int_0^{\infty} \frac{i k^3 \cos \theta e^{-2k f}}{k - k_o \sec^2 \theta - iv \sec \theta} dk d\theta \right]$$

$$+ m \left(\frac{2}{a^3} + \frac{1}{|a^2 + 4f^2|^{3/2}} - \frac{3a^2}{|a^2 + 4f^2|^{5/2}} \right)$$

$$+ \operatorname{Re} \left[\frac{k_o m}{\pi} \int_{-\pi}^{\pi} \int_0^{\infty} \frac{k^2 e^{-k(i a \cos \theta + 2f)}}{k - k_o \sec^2 \theta - iv \sec \theta} dk d\theta \right] \quad [9]$$

The integral with respect to k can be evaluated using the contour integral as in Equation [11]. After the integration, v is set equal to zero. Then the first integral can be represented by means of modified Bessel's functions (see Lunde 1952) as in Equation [15] i.e.

$$\operatorname{Re} \int_{-\pi}^{\pi} \int_0^{\infty} \frac{i k^3 \cos \theta e^{-2k f}}{k - k_o \sec^2 \theta - iv \sec \theta} dk d\theta = -\pi k_o^3 e^{-k_o f}$$

$$\times \left\{ K_o(k_o f) + \left(1 + \frac{1}{2k_o f} \right) K_1(k_o f) \right\}$$

4. NONDIMENSIONAL FORM

We may use the relation between μ and the radius of the sphere b in a uniform stream at infinite depth

$$\mu = \frac{V}{2} b^3$$

Similarly

$$m = \frac{V}{4} r^2$$

where r is the maximum radius of a half body produced by a source in a uniform stream.

Then in the nondimensional form as

$$\bar{R}_1 = \frac{R}{\frac{\pi}{2} \rho V^2 r^2} , \quad \bar{b} = \frac{b}{f} , \quad F_f = \frac{V}{\sqrt{gf}} = \text{Froude number, etc.}$$

$$\bar{a} = \frac{a}{f} , \quad \bar{k}_0 = k_0 f = \frac{gf}{V^2} = \frac{1}{F_f^2} , \quad \bar{r} = \frac{r}{f} ,$$

and dropping bars for convenience we have

$$\begin{aligned} R_1(-a, 0, -1) = & -b^3 \left(\frac{2}{a^3} + \frac{1}{(a^2 + 4)^{3/2}} - \frac{3a^2}{(a^2 + 4)^{5/2}} \right) \\ & + \frac{2b^6}{F_f^8 r^2} e^{-k_0} \left\{ K_0(k_0) + \left(1 + \frac{1}{2k_0} \right) K_1(k_0) \right\} \\ & - \text{Re} \frac{2b^3}{\pi F_f^2} R_0 \end{aligned} \quad [10]$$

where K_0 and K_1 represent the zero order and first order modified Bessel functions of the 2nd kind respectively, and

$$R_o = \operatorname{Re} \int_{-\pi}^{\pi} \int_0^{\infty} \frac{k^2 e^{-k(ia \cos \theta + 2f)} dk d\theta}{k - k_o \sec^2 \theta - iv \sec \theta} \quad [11]$$

5. EVALUATION OF INTEGRAL R_o

Taking a contour as shown in Figure 2 for the integration of (1) with respect to k and, noting that $v > 0$ for the residue at the singularity $k = k_o \sec^2 \theta + v \sec \theta$ and later letting $v \rightarrow 0$. We obtain

$$R_o = 2\pi \int_{-\pi/2}^{\pi/2} k_o^2 \sec^4 \theta e^{-2k_o f \sec^2 \theta} \sin(ak_o \sec \theta) d\theta$$

$$+ \int_0^{\infty} \int_{-\pi}^{\pi} \frac{(k_o \sec^2 \theta + it) t^2 e^{-2itf} \sinh(\operatorname{at} \cos \theta) d\theta dt}{t^2 + k_o^2 \sec^4 \theta}$$

The second integral of the right hand side can be shown to vanish because of the odd function, \sinh .

Hence

$$\frac{F_f^4 R_o}{2\pi} = \int_0^{\pi/2} e^{-2k_o \sec^2 \theta} \sec^4 \theta \sin(ak_o \sec \theta) d\theta$$

$$\equiv R_i [ak_o, k_o, 4] \quad [12]$$

If we expand $\sin(ak_o, \sec \theta)$ into a series of $ak_o \sec \theta$,

$$Ri[ak_o, k_o, 4] = \int_0^{\pi/2} e^{-2k_o \sec^2 \theta} \sum_{n=0}^{\infty} (-1)^n \frac{(ak_o)^{2n+1}}{(2n+1)} \times \sec^{2n+5} \theta d\theta \quad [13]$$

To evaluate the integral

$$I_v \equiv \int_0^{\pi/2} e^{-2k_o \sec^2 \theta} \sec^{2v+1} \theta d\theta \quad [14]$$

we put $\sec \theta = \cosh \frac{u}{2}$ and obtain

$$I_v = \frac{e^{-k_o}}{2} \int_0^{\infty} e^{-k_o \cosh u} \left(\frac{1 + \cosh u}{2} \right)^v d u \equiv \frac{e^{-h}}{2^{v+1}} G_v(k_o)$$

$$G_1(k_o) = \int_0^{\infty} e^{-k_o \cosh u} (1 + \cosh u) du = K_o(k_o) - K_o'(k_o) \quad [15]$$

where $K_o'(k_o) = \frac{d K_o(k_o)}{d k_o} = -K_1(k_o)$. In addition we can

prove easily

$$G_n(k_o) = \int_0^{\infty} e^{-k_o \cosh u} (1 + \cosh u)^n du$$

$$\equiv G_{n-1}(k_o) - G_{n-1}'(k_o) \quad [16]$$

Hence we get

$$I_v = \frac{e^{-k_o}}{2^v + 1} \left\{ K_o(k_o) - K_o'(k_o) \right\}_{(n)}$$

where

$$\left\{ K_o(k_o) - K_o'(k_o) \right\}_{(n)} \equiv K_o(k_o) - \binom{n}{1} \frac{dK_o(k_o)}{dh} \\ + \binom{n}{2} \frac{d^2 K_o(k_o)}{dh^2} - \dots + (-1)^n \frac{d^n K_o(k_o)}{dh^n} \quad [17]$$

We now perform the integration of [13] term by term and obtain

$$R_i(ak_o, k_o, 4) = \sum_{n=0}^{\infty} (-1)^n \frac{(ak_o)^{2n+1}}{(2n+1)!} I_{n+2} \\ = \frac{e^{-k_o}}{2} \sum_{n=0}^{\infty} \frac{(-1)^n (ak_o)^{2n+1}}{(2n+1)! 2^{n+2}} \left\{ K_o(k_o) - K_o'(k_o) \right\}_{(n+2)} \quad [18]$$

This series is proved to be convergent for any ak_o and $k_o > 0$ (see appendix). When ak_o is sufficiently small this series converges rapidly. In computations, the following recurrence relations are of great value.

$$G_n(h) = \left(2 + \frac{n-1}{h} \right) G_{n-1}(h) - \frac{(2n-3)}{h} G_{n-2}(h) \quad [19]$$

for all integers n . This can be easily proved by integrating Equation [15] by parts. In addition

$$\begin{aligned} G_0(h) &= K_0(h) \\ G_1(h) &= K_0(h) + K_1(h) \end{aligned} \quad [20]$$

On inserting the value of R_0 obtained by the foregoing procedure into Equation [10] we finally obtain the non dimensional, horizontal component of the force at the doublet.

6. FORCE AT SOURCE POINT

Similarly, the force at point $(0,0,-f)$ is obtained from [2] in dimensional form

$$\begin{aligned} \left(\frac{\partial \phi}{\partial x} \right)_{0,0,-f} &= -\mu \left[\frac{\partial}{\partial x} \left\{ \frac{1}{(x+a)^2} - \frac{x+a}{\{(x+a)^2 + (z-f)^2\}^{3/2}} \right\} \right. \\ &\quad \left. + \operatorname{Re} \frac{k_0}{\pi} \frac{\partial}{\partial x} \int_{-\pi}^{\pi} \int_0^{\infty} \frac{ik \sec \theta e^{k(i\omega + z-f)} dk d\theta}{k - k_0 \sec^2 \theta - iv \sec \theta} \right]_{0,0-f} \\ &= \mu \left\{ \frac{2}{a^3} + \frac{1}{(a^2+4f^2)^{3/2}} - \frac{3a^2}{(a^2+4f^2)^{5/2}} \right\} \\ &\quad + \operatorname{Re} \frac{k_0 \mu}{\pi} \int_{-\pi}^{\pi} \int_0^{\infty} \frac{k^2 e^{k(i\omega + z-f)} dk d\theta}{k - k_0 \sec^2 \theta - iv \sec \theta} \end{aligned}$$

$$\begin{aligned}
 \left(\frac{\partial \phi_{20}}{\partial x} \right)_{0,0,-f} &= \operatorname{Re} \frac{k_o m}{\pi} \int_{-\pi}^{\pi} \int_0^{\infty} \frac{ik \sec \theta e^{-2kf} dk d\theta}{k - k_o \sec^2 \theta - iv \sec \theta} \\
 &= k_o^2 m \left\{ K_o(k_o f) + K_1(k_o f) \right\} \\
 R_2(0,0,-f) &= 4 \pi \rho m \left(\frac{\partial \phi_1}{\partial x} + \frac{\partial \phi_{20}}{\partial x} \right)_{0,0,-f}
 \end{aligned}$$

The integrals are evaluated exactly in the same way as in Sections 3-5.

7. TOTAL FORCE AND OPTIMUM PARAMETERS

The total force, or the total wave resistance is, in nondimensional form,

$$\begin{aligned}
 R &= R_1(-a,0,-1) + R_2(0,0,-1) \\
 &= e^{-k_o} \left[\frac{2b^6}{r^2 F_f^3} \left\{ K_o(k_o) + \left(1 + \frac{1}{2k_o} \right) K_1(k_o) \right\} \right. \\
 &\quad \left. + \frac{r^2}{2F_f^4} \left\{ K_o(k_o) + K_1(k_o) \right\} \right] - \frac{8b^3}{F_f^6} \operatorname{Ri}[ak_o, k_o, 4] \quad [21]
 \end{aligned}$$

where $\operatorname{Ri}(ak_o, k_o, 4)$ is given by Equation [18]. We may write alternatively

$$R = R_s + R_b + R_{int}$$

where the nondimensional wave resistance (or wave resistance coefficient) due to a source

$$R_s = \frac{e^{-k_o}}{2 F_f^4} \left\{ K_o(k_o) + K_1(k_o) \right\}$$

and due to a doublet

$$R_b = 2e^{-k_o} \frac{b^6}{F_f^8} \left\{ K_o(k_o) + \left(1 + \frac{1}{2k_o} \right) K_1(k_o) \right\}$$

and the interference term

$$R_{int} = - \frac{8}{F_f^6} b^3 R_i [ak_o, k_o, 4]$$

Hence $R_b + R_{int}$ is the total influence of the bulb. To obtain the optimum value of the distance a which makes R minimum we notice that $R_i(ak_o, k_o, 4)$ is the only function of a appearing in the right hand side of the above Expression [21]. The optimum value of a is readily obtained from Equation [18] with the aid of a numerical - graphical procedure.

The optimum value of b was obtained by differentiating R with respect to b , putting it equal to zero, and solving for b .

$$\frac{b}{\sqrt[3]{r^2}} = - \sqrt[3]{a} \frac{2F_f^2 R_i [ak_o, k_o, 4]}{K_o(k_o) + \left(1 + \frac{1}{2k_o} \right) K_1(k_o)} \quad [22]$$

The optimum values of a and $br^{2/3}$ thus obtained are plotted against F_f^2 in Figure 4.

8. REMARKS

With these optimum values of a and b , R/r^2 is plotted in Figure 3 versus F^2 . Here we can see that a considerable reduction in the wave resistance is obtained by using an optimum bulb. The force at the point of the doublet in the presence of the source with optimum values of a and b is also plotted in Figure 3. We can see there that the favorable effect of the bulb is due to the pulling force (negative) at the doublet. The force at the point source in the presence of the doublet is not shown there, but obviously it is a positive force, which is the sum of the absolute value of force at the doublet point and the net force which are both shown in Figure 3. This reveals that the reduction of force on the half body - bulb combination is entirely achieved by the creation of a large bulb thrust and not by the reduction of resistance on the half-body itself. In fact, the wave resistance of the half-body by itself would appear to increase in the presence of the bulb.

The wave resistance of a source has a singularity at $f=0$. The wave resistance coefficient C_w increases as f/r decreases by the factor $(f/r)^2$ at a fixed Froude number as shown in Figure 3 or Equation [10]. Although the shape of the body formed by a source near the surface looks more like a ship shape, this singularity prevents us from approaching it in this way.

From the radius of the bulb b shown in Figure 4 we obtain the strength of the doublet $\mu = V b^3/2$. This relation is used only for approximating the size of bulb. The doublet here by no means results in a sphere. There is not only the influence of the free surface but also that of the source to alter its shape from that of the sphere. The form of the body will be discussed in Section 14 later. Although the distance, a, between the doublet and the source seems to be large compared to b it is highly probable that the resulting bulb and bow are connected by faired lines (See Figure 9A).

CASE II

9. WAVE HEIGHTS

We now consider the same problem as in Case I except that the point source is replaced by a vertical line source extending from the free surface to depth d . In order to find the wave resistance it is now more convenient to use Havelock's formula, (Havelock, 1934) rather than Logally's theorem. With the former method it is necessary to determine the wave height at a large distance down-stream of the body.

As shown in Equation [8] the x component of perturbed velocity of the flow due to a point source at depth f_1 with strength m is for large x

$$\left(\frac{\partial \phi}{\partial x}\right)_{x,y,0} = -\frac{mk_0}{\pi} \operatorname{Re} \int_{-\pi}^{\pi} \int_0^{\infty} \frac{i k \sec \theta e^{k(i\omega_1 - f_1)}}{k - k_0 \sec^2 \theta - iv \sec \theta} dk d\theta \quad [23]$$

$$\text{where } \omega_1 = x \cos \theta + y \sin \theta$$

Hence, if we consider a vertical source line with uniform strength m_1 per unit length, (or $m=m_1 d$), then on the free surface we have for large x

$$\begin{aligned} \left. \frac{\partial \phi}{\partial x} \right|_{x,y,0} &= - \frac{m_1 k_0}{\pi} \operatorname{Re} \int_0^d \int_{-\pi}^{\pi} \int_0^{\infty} \frac{i k \sec \theta e^{k(i\omega_1 - f_1)}}{k - k_0 \sec^2 \theta - iv \sec \theta} dk d\theta df_1 \\ &= \frac{mk_0}{\pi} \operatorname{Re} \int_{-\pi}^{\pi} \int_0^{\infty} \frac{(e^{-1} - 1) i \sec \theta e^{-kd}}{k - k_0 \sec^2 \theta - iv \sec \theta} dk d\theta \\ &= 8 m_1 k_0 \int_0^{\pi/2} (1 - e^{-k_0 d \sec^2 \theta}) \sec \theta \cos (k_0 x \sec \theta) \\ &\quad \times \cos (k_0 y \sin \theta \sec^2 \theta) d\theta \end{aligned} \quad [24]$$

using contour integration as was done in [11] and [12]. Hence the wave height far from the source line is, from [5] with

$$v_1 = 0$$

$$\begin{aligned} \zeta_s &= 8 \frac{m_1}{V} \int_0^{\pi/2} (1 - e^{-k_0 d \sec^2 \theta}) \sec \theta \cos (k_0 x \sec \theta) \\ &\quad \times \cos (k_0 y \sin \theta \sec^2 \theta) d\theta \end{aligned} \quad [25]$$

Similarly, the wave height due to a doublet at $(-a, 0, -f)$ is,
for large x

$$\zeta_b = - \frac{8k_o^2 \mu}{V} \int_0^{\pi/2} \sec^4 \theta e^{-k_o f \sec^2 \theta} [\sin(k_o x \sec \theta) \cos(k_o a \sec \theta) + \cos(k_o x \sec \theta) \sin(k_o a \sec \theta)] \cos(k_o y \sin \theta \sec^2 \theta) d\theta \quad [26]$$

10. HAVELOCK'S FORMULA AND WAVE RESISTANCE

Suppose the wave height at large x ,

$$\zeta = \int_0^{\pi/2} (P_1 \sin A \cos B + P_2 \cos A \sin B + P_3 \cos A \cos B + P_4 \sin A \sin B) d\theta \quad [27]$$

where $A = k_o x \sec \theta$. $B = k_o y \sin \theta \sec^2 \theta$. P_i is a function of θ and other physical parameters. Then Havelock's formula (1934) for wave resistance is given by

$$R = \frac{1}{4} \rho \pi V^2 \int_0^{\pi/2} (P_1^2 + P_2^2 + P_3^2 + P_4^2) \cos^3 \theta d\theta \quad [28]$$

Hence in our case $\zeta = \zeta_s + \zeta_b$ and

$$\begin{aligned}
 R = 16 \rho \pi \int_0^{\pi/2} & [k_o^4 \mu^2 e^{-2k_o f \sec^2 \theta} \frac{-k_o d \sec^2 \theta}{\sec^5 \theta + m_1^2 (1 - e^{-k_o d \sec^2 \theta})^2 \cos \theta} \\
 & - 2k_o^2 m_1 \mu e^{-k_o f \sec^2 \theta} \frac{-k_o d \sec^2 \theta}{(1 - e^{-k_o d \sec^2 \theta}) \sec^2 \theta \sin(k_o a \sec \theta)}] d\theta \\
 \equiv & R_b + R_{ls} + R_{li}
 \end{aligned} \tag{29}$$

where the resistance due to the bulb is

$$\begin{aligned}
 R_b = 16 \rho \pi k_o^4 \mu^2 \int_0^{\pi/2} & e^{-k_o f \sec^2 \theta} \frac{\sec^5 \theta}{\sec^5 \theta} d\theta \\
 = 4 \pi \rho e^{-k_o f} k_o^4 \mu^2 & \left\{ K_o(k_o f) + \left(1 + \frac{1}{2k_o f} \right) K_1(k_o f) \right\}
 \end{aligned}$$

from Equations [14] - [17] where K_o , K_1 , modified Bessel func-

tions of the second kind. The resistance due to the line source is

$$\begin{aligned}
 R_{ls} = 16 \rho \pi m_1^2 \int_0^{\pi/2} & (1 - e^{-k_o d \sec^2 \theta})^2 \cos \theta d\theta \\
 = 16 \rho \pi m_1^2 & \left[1 - k_o d e^{-k_o d/2} \left\{ K_1(k_o d/2) - K_o(k_o d/2) \right\} \right. \\
 & \left. + k_o e^{-k_o d} \left\{ K_1(k_o d) - K_o(k_o d) \right\} \right]
 \end{aligned}$$

and the resistance due to the interaction between the bulb and the line source is

$$R_{\ell 1} = -32 \rho \pi k_o^2 m_1 \mu \int_0^{\pi/2} e^{-k_o f} \sec^2 \theta \left(\frac{1}{1-e^{-k_o d}} \sec^2 \theta \right) \times \sec^2 \theta \sin (k_o a \sec \theta) d\theta \quad [30]$$

which can be evaluated by a series expansion as in Section 6.

11. NONDIMENSIONAL FORM

If we put

$$m_1 = \bar{m} \frac{Vd}{4} \quad \mu = \frac{Vb^3}{2} \quad [31]$$

where \bar{m} is a nondimensional coefficient, we nondimensionalize with respect to d , e.g.

$$C_w = \bar{R} = \frac{R}{\frac{\pi}{2} \rho V^2 d^2}, \quad F_d = \frac{V}{\sqrt{gd}}, \quad \bar{k}_o = k_o d, \quad \bar{f} = \frac{f}{d},$$

$$\bar{b} = \frac{b}{d}, \quad \bar{a} = \frac{a}{d} \quad [32]$$

and dropping bars for convenience we obtain

$$R_b = \frac{2b^6}{F_d^3} e^{-k_o f} \left\{ K_o (k_o f) + \left(1 + \frac{1}{2k_o f} \right) K_1 (k_o f) \right\} \quad [33]$$

$$R_{\ell s} = 2 m^2 \left[1 - k_o e^{-k_o/2} \left\{ K_1 \left(\frac{k_o}{2} \right) - K_o \left(\frac{k_o}{2} \right) \right\} + k_o e^{-k_o} \times \left\{ K_1 (k_o) - K_o (k_o) \right\} \right] \quad [34]$$

$$R_{\ell 1} = -8m \frac{b^3}{F_d^4} \int_0^{\pi/2} e^{-k_o f} \sec^2 \theta \left(\frac{1}{1-e^{-k_o \sec^2 \theta}} \right) \sec^2 \theta \times \sin (k_o a \sec \theta) d\theta \quad [35]$$

If we use the notation in Section 5

$$R_{\ell i} = - \frac{b^3}{F_d^4} \left\{ R_i \left[a k_o, \frac{k_o f}{2}, 2 \right] - R_i \left[a k_o, \frac{k_o (f+1)}{2}, 2 \right] \right\} [36]$$

$$R = R_b + R_{\ell s} + R_{\ell i} [29]$$

$R_{\ell i}$ is an oscillating function of $k_o a$, and if we apply the method of stationary phase (see e.g. Lamb, 1945, p. 395) we know that it behaves like

$$e^{-k_o f} \left(1 - e^{-k_o} \right) \sin \left(k_o a + \frac{\pi}{4} \right) [38]$$

when $k_o a$ is large.

When $k_o a$ is sufficiently small, $R_{\ell i}$ is always negative because of the property of the function R_i in Section 5.

12. OPTIMUM PARAMETERS

In this first mode of the function $R_{\ell i}$ the optimum value of a is obtained by finding the stationary value of $R_{\ell i}$ by the graphical method as in Case I. The optimum value of b is obtained easily as in Case I, since R is a polynomial with respect to b ,

$$b^3 = \frac{2 F_d^4 m \int_{\pi/2}^{\infty} e^{-k_o f} \sec^2 \theta \left(1 - e^{-k_o d} \sec^2 \theta \right) \sec^2 \theta \sin \left(k_o a \sec \theta \right) d\theta}{e^{-k_o f} \left[K_o (k_o f) + \left(1 + \frac{1}{2 k_o f} \right) K_1 (k_o f) \right]} [39]$$

Then the total effect of the bulb of this size on the wave resistance becomes

$$R_b + R_{\ell i} = -8m^2 \frac{\left[\int_0^{\pi/2} e^{-k_0 f} \sec^2 \theta \left(\frac{1}{1-e^{-k_0 d} \sec^2 \theta} \right) \sec^2 \theta \sin(k_0 a \sec \theta) d\theta \right]^2}{e^{-k_0 f} \left[K_0(k_0 f) + 1 + \frac{1}{2k_0 f} K_1(k_0 f) \right]} \quad [40]$$

The graphs of the optimum value of a and the optimum value of $b/\sqrt[3]{m}$ for the obtained optimum value of a are plotted with respect to F_d^2 for several values of f , the depth of the doublet, in Figures 6 and 7. R/m^2 , $(R_b + R_{\ell i})/m^2$, and $R_{\ell s}/m^2$ are plotted versus F_d^2 , taking the optimum values of a and b for each F_d^2 in Figure 5.

13. SHIP SHAPES

From the boundary condition [6], we can see that the free surface behaves like a solid wall when the velocity V is small (if $F_L < .3$, $\frac{1}{k_0 L} < .09$ in Equation [6]). Inui (1957) found by comparing his experimental results with theoretical analyses that the effect of assuming that the free surface acts like a solid wall, when computing the stream surface generated by a given singularity distribution, led to negligible error up to a Froude number of $F_L = 0.7$. Accordingly we have for the potential due to the source line and its mirror image:

$$\phi_s = \int_{-d}^d \frac{m_1 df}{\sqrt{x^2 + y^2 + (z-f)^2}} = m_1 \log \left(\frac{z+d + \sqrt{x^2 + y^2 + (z+d)^2}}{z-d + \sqrt{x^2 + y^2 + (z-d)^2}} \right).$$

For the doublet

$$\phi_d = -\mu(x+a) \left(\frac{1}{\{(x+a)^2+y^2+(z+f)^2\}^{3/2}} + \frac{1}{\{(x+a)^2+y^2+(z-f)^2\}^{3/2}} \right)$$

Considering a sink line from point $(L, 0, 0)$ to point $(L, 0, -d)$ in addition to the doublet-source-line system we find for the total velocity components,

$$u = -\frac{\partial \phi}{\partial x} + V, \quad v = -\frac{\partial \phi}{\partial y}, \quad w = -\frac{\partial \phi}{\partial z}.$$

Then the streamline equations are

$$\frac{dx}{u} = \frac{dy}{v} = \frac{dz}{w}.$$

We solve this by Runge-Kutta-Gill's (Runge, 1895; Kutta, 1901; Gill, 1951; or see Ralston and Wilf, 1960) numerical method to obtain the three dimensional streamlines starting from the stagnation points. Figures 9-11 show the body streamlines represented by three special cases of different singularity distributions respectively: viz. a point doublet, a source line, and a sink line with the three different sets of parameters. Figure 17 shows the case of the doublet line discussed in Case III. Each of these figures shows the projections of the several body streamlines on the x y plane and the x z plane. The calculations were performed on the IBM 1620. In making these computations it was necessary to exercise extreme care in the selection of interval increments at the neighborhood of the stagnation point and in the vicinity of large curvature. The resulting body streamlines are smooth curves with a hollow place although the distance between the doublet and the source appears to be

too large to be a single connected body.

14. DISCUSSION

The optimum distance between the doublet and the source line, and the optimum size of the bulb increase with the flow speed and depth of the doublet as shown in Figures 6 and 7. However, the depth effect of the doublet on the wave resistance decreases with flow speed as long as we take the optimum bulb size and the optimum distance between the doublet and the source line at each selected depth. This is shown in Figure 8.

The size of bulb is considerably large for the reasonably high Froude number. When $F_d^2 > 2$ the width of the bulb becomes larger than the beam length as shown in Figures 7 and 10. Hence the bulb may be considered rather as a blunt bow of ship than an appendage. However, as we notice in Figures 10 - 11, the hollow place between the bulb and ship body may contribute to the flow separation.

Assuming no serious separation takes place the reduction of the wave resistance due to the bulb is remarkably great. Figure 5 shows that the effect of an optimum bulb is to reduce the wave resistance by more than 60 percent of that contributed by the line source alone at all Froude numbers.

The wave resistance coefficient of the source line bow alone is also shown in Figure 5. It has a jump at $F_d = 0$, and it decreases as F_d increases. Since this is a nondimensional quantity it does not mean that the wave resistance itself has a jump at $F_d = 0$.

CASE III

15. WAVE RESISTANCE OF THE SYSTEM OF A DOUBLET LINE AND A SOURCE LINE

As shown in Case II the optimum size of the bulb is remarkably large, especially for higher Froude numbers. We will now investigate the result when the doublet strength is distributed linearly along the vertical line from $(-a, 0, -f_1)$, to $(-a, 0, -f_2)$ in front of the same source line as in Case II.

If we take $\mu = \mu_1 + f\mu_2$ for the doublet strength per unit length, we have for the wave height far behind the system due to the bulb, from Equation [26]

$$\begin{aligned}
 \zeta_b = & - \frac{8k_o^2}{V} \int_0^{\pi/2} \int_{f_1}^{f_2} e^{-k_o f \sec^2 \theta} (\mu_1 + \mu_2 f) \sec^4 \theta \\
 & \times [\sin (k_o x \sec \theta) \cos (k_o a \sec \theta) + \cos (k_o x \sec \theta) \\
 & \times \sin (k_o a \sec \theta)] \cos (k_o y \sin \theta \sec^2 \theta) d f d \theta \\
 = & - \frac{8}{V} \int_0^{\pi/2} \left[k_o \sec^2 \theta \left\{ e^{-k_o f_1 \sec^2 \theta} (\mu_2 f_1 + \mu_1) - e^{-k_o f_2 \sec^2 \theta} \right. \right. \\
 & \times (\mu_2 f_2 + \mu_1) \left. \left. \right\} + \mu_2 \left(e^{-k_o f_1 \sec^2 \theta} - e^{-k_o f_2 \sec^2 \theta} \right) \right] \\
 & \times [\sin (k_o x \sec \theta) \cos (k_o a \sec \theta) + \cos (k_o x \sec \theta) \\
 & \times \sin (k_o a \sec \theta)] \cos (k_o y \sin \theta \sec^2 \theta) d \theta \quad [41]
 \end{aligned}$$

and due to the source line, from Equation [25]

$$\zeta_s = \frac{8m_1}{V} \int_0^{\pi/2} \left(1 - e^{-k_0 d \sec^2 \theta} \right) \sec \theta \cos [k_0 x \sec \theta] \times \cos (k_0 y \sin \theta \sec^2 \theta) d\theta \quad [25]$$

Using Havelock's formula (27) and (28), we have for the total wave resistance, due to the doublet and source lines

$$R = 16 \pi \rho \int_0^{\pi/2} \left(\frac{m_1^2}{2} \left(1 - e^{-k_0 d \sec^2 \theta} \right)^2 \cos \theta + k_0^2 \sec \theta \left\{ e^{-2k_0 f_1 \sec^2 \theta} \left(\frac{\mu_2 f_1 + \mu_1}{\mu_2 f_1 + \mu_1} \right)^2 + e^{-2k_0 f_2 \sec^2 \theta} \left(\frac{\mu_2 f_2 + \mu_1}{\mu_2 f_2 + \mu_1} \right)^2 - 2 e^{-k_0 (f_1 + f_2) \sec^2 \theta} \left(\frac{\mu_2 f_1 + \mu_1}{\mu_2 f_1 + \mu_1} \right) \left(\frac{\mu_2 f_2 + \mu_1}{\mu_2 f_2 + \mu_1} \right) \right\} + 2k_0 \times \left[e^{-2k_0 f_1 \sec^2 \theta} \left(\frac{\mu_2 f_1 + \mu_1}{\mu_2 f_1 + \mu_1} \right) \mu_2 + e^{-2k_0 f_2 \sec^2 \theta} \left(\frac{\mu_2 f_2 + \mu_1}{\mu_2 f_2 + \mu_1} \right) \mu_2 - e^{-k_0 (f_1 + f_2) \sec^2 \theta} \left\{ \frac{2\mu_1 \mu_2 + \mu_2^2}{\mu_1^2 + \mu_2^2} (f_1 + f_2) \right\} \right] \cos \theta + \mu_2^2 e^{-2k_0 f_1 \sec^2 \theta} \cos^3 \theta + \mu_2^2 e^{-2k_0 f_2 \sec^2 \theta} \cos^3 \theta - 2\mu_2^2 \times e^{-k_0 (f_1 + f_2) \sec^2 \theta} \cos^3 \theta + \left[-2k_0 m_1 \left\{ e^{-k_0 f_1 \sec^2 \theta} (f_1 \mu_2 + \mu_1) - e^{-k_0 f_2 \sec^2 \theta} (f_2 \mu_2 + \mu_1) \right\} + 2k_0 m_1 \left\{ e^{-k_0 (f_1 + d) \sec^2 \theta} (f_1 \mu_2 + \mu_1) - e^{-k_0 (f_2 + d) \sec^2 \theta} (f_2 \mu_2 + \mu_1) \right\} - 2m_1 \mu_2 \cos^2 \theta \left(e^{-k_0 f_1 \sec^2 \theta} - e^{-k_0 f_2 \sec^2 \theta} \right) - e^{-k_0 (f_1 + d) \sec^2 \theta} + e^{-k_0 (f_2 + d) \sec^2 \theta} \right] \sin (k_0 a \sec \theta) \right) d\theta \quad [42]$$

16. NONDIMENSIONAL FORM

We perform the integrations using the methods taken in Equations [11], [15], and [16], and nondimensionalize physical variables with respect to m_1 and d as in Case II, i.e.

$$C_w = \bar{R} = \frac{R}{\frac{\pi}{2} \rho m^2 V^2 d^2}, \quad \bar{\mu}_1 = \frac{\mu_1}{m_1 d_1}, \quad \bar{\mu}_2 = \frac{\mu_2}{m_1}, \quad \bar{m}_1 = \frac{\bar{m} V d}{4},$$

$$F_d = \frac{V}{\sqrt{gd}}, \quad \bar{k}_o = k_o d, \quad \bar{f}_1 = f_1/d, \quad \bar{f}_2 = f_2/d \quad [43]$$

and dropping bars for convenience we obtain

$$R = R_{ls} + R_{lb} + R_{lli}$$

$$R_{ls} = 2 \left[1 - k_o \left\{ K_1 \left(\frac{k_o}{2} \right) - K_o \left(\frac{k_o}{2} \right) e^{-k_o/2} + k_o e^{-k_o} \left\{ K_1(k_o) - K_o(k_o) \right\} \right\} \right] \quad [44]$$

$$R_{lb} = \frac{2}{F_d^4} \left[\frac{e^{-k_o f_1}}{2} K_o(k_o f_1) (\mu_2 f_1 + \mu_1)^2 + \frac{e^{-k_o f_2}}{2} \right.$$

$$\times K_o(k_o f_2) (\mu_2 f_2 + \mu_1)^2 - e^{-k_o(f_1+f_2)/2} K_o \left(\frac{k_o(f_1+f_2)/2}{2} \right) (\mu_2 f_1 + \mu_1) (\mu_2 f_2 + \mu_1) \left. \right]$$

$$+ \frac{4}{F_d^2} \left[k_o f_1 e^{-k_o f_1} \left\{ K_1(k_o f_1) - K_o(k_o f_1) \right\} (\mu_1 f_1 + \mu_1) \mu_2 \right.$$

$$+ k_o f_2 e^{-k_o f_2} \left\{ K_1(k_o f_2) - K_o(k_o f_2) \right\} (\mu_2 f_2 + \mu_1) \mu_2$$

$$- \frac{k_o(f_1+f_2)}{2} e^{-k_o(f_1+f_2)/2} \left\{ K_1 \left(\frac{k_o(f_1+f_2)/2}{2} \right) - K_o \left(\frac{k_o(f_1+f_2)/2}{2} \right) \right\}$$

$$\times \left. \left[2\mu_1 \mu_2 + \mu_2^2 (f_1 + f_2) \right] \right] + \frac{4}{3} \mu_2^2 \left[e^{-k_o f_1} \left\{ 2k_o f_1 K_o(k_o f_1) - (2k_o f_1 - 1) K_1(k_o f_1) \right\} k_o f_1 \right.$$

$$+ e^{-k_o f_1} k_o f_2 \left\{ 2k_o f_2 K_o(k_o f_2) - (2k_o f_2 - 1) K_1(k_o f_2) \right\}$$

$$- e^{-k_o(f_1+f_2)/2} k_o(f_1+f_2) \left\{ k_o(f_1+f_2) \right.$$

$$\times K_o \left(\frac{k_o(f_1+f_2)/2}{2} \right) - \left(k_o(f_1+f_2) - 1 \right) K_1 \left(\frac{k_o(f_1+f_2)/2}{2} \right) \left. \right] \quad [45]$$

$$\begin{aligned}
 R_{\ell\ell i} = & - \frac{4}{F_d^2} \left\{ (f_1 \mu_2 + \mu_1) \left(\text{Ri} \left[ak_o, \frac{k_o f_1}{2}, 0 \right] - \text{Ri} \left[ak_o, \frac{k_o (f_1+1)}{2}, 0 \right] \right) \right. \\
 & - (f_2 \mu_2 + \mu_1) \left(\text{Ri} \left[ak_o, \frac{k_o f_2}{2}, 0 \right] - \text{Ri} \left[ak_o, \frac{k_o (f_2+1)}{2}, 0 \right] \right) \\
 & - 4 \mu_2 \left\{ \text{Ri} \left[ak_o, \frac{k_o f_1}{2}, -2 \right] - \text{Ri} \left[ak_o, \frac{k_o f_2}{2}, -2 \right] \right. \\
 & \left. \left. - \text{Ri} \left[ak_o, \frac{k_o (f_1+1)}{2}, -2 \right] + \text{Ri} \left[ak_o, \frac{k_o (f_2+1)}{2}, -2 \right] \right\} \quad [46]
 \end{aligned}$$

$$\text{where } \text{Ri} [g, k, n] = \int_0^{\pi/2} e^{-2k \sec^2 \theta} \sec^n \theta \sin (g \sec \theta) d\theta$$

which is defined in Expression [12], and is evaluated in Equations [12] - [18] by the series expansion in g .

17. OPTIMUM PARAMETERS

The optimum values of μ_1 and μ_2 which make $R_{\ell b} + R_{\ell\ell i}$ minimum may be obtained by the usual methods. We differentiate R partially with respect to μ_1 and μ_2 respectively, put the results equal to zero, and solve the resulting two simultaneous equations for the optimum values of μ_1 and μ_2 . The equations for μ_1 and μ_2 resulting from the above mentioned differentiation are

$$\mu_1 = \frac{Y_1 - \mu_2 X}{W_1}, \quad \mu_2 = \frac{Y_2 - \mu_1 X}{W_2} \quad [47]$$

where

$$X = - \frac{1}{F_d^4} \left[e^{-k_o f_1} K_o(k_o f_1) f_1 + e^{-k_o f_2} K_o(k_o f_2) f_2 \right.$$

$$\left. - e^{-k_o(f_1+f_2)/2} K_o\left(\frac{(k_o(f_1+f_2)/2)}{2}\right) (f_1+f_2) \right]$$

$$+ \frac{2}{F_d^4} \left[e^{-k_o f_1} K_1(k_o f_1) f_1 + e^{-k_o f_2} K_1(k_o f_2) f_2 \right.$$

$$\left. - e^{-k_o(f_1+f_2)/2} K_1\left(\frac{(k_o(f_1+f_2)/2)}{2}\right) (f_1+f_2) \right]$$

$$Y_1 = \frac{2}{F_d^4} \left\{ \text{Ri} \left[ak_o, \frac{k_o f}{2}, 0 \right] - \text{Ri} \left[ak_o, \frac{k_o(f+1)}{2}, 0 \right] - \text{Ri} \left[ak_o, \frac{k_o f_2}{2}, 0 \right] \right.$$

$$\left. + \text{Ri} \left[ak_o, \frac{k_o(f_2+1)}{2}, 0 \right] \right\}$$

$$Y_2 = \frac{2}{F_d^2} \left[f_1 \left\{ \text{Ri} \left[ak_o, \frac{k_o f_1}{2}, 0 \right] - \text{Ri} \left[ak_o, \frac{k_o(f_1+1)}{2}, 0 \right] \right\} \right.$$

$$\left. - f_2 \left\{ \text{Ri} \left[ak_o, \frac{k_o f_2}{2}, 0 \right] - \text{Ri} \left[ak_o, \frac{k_o(f_2+1)}{2}, 0 \right] \right\} \right] + 2 \left\{ \text{Ri} \left[ak_o, \frac{k_o f_1}{2}, -2 \right] \right.$$

$$\left. - \text{Ri} \left[ak_o, \frac{k_o f_1}{2}, -2 \right] - \text{Ri} \left[ak_o, \frac{k_o(f_1+1)}{2}, -2 \right] + \text{Ri} \left[ak_o, \frac{k_o(f_2+1)}{2}, -2 \right] \right\}$$

$$W_1 = \frac{1}{F_d^4} \left[e^{-k_o f_1} K_o(k_o f_1) + e^{-k_o f_2} K_o(k_o f_2) - 2 e^{-k_o(f_1+f_2)/2} \right.$$

$$\left. \times K_o\left(\frac{k_o(f_1+f_2)}{2}\right) \right]$$

$$\begin{aligned}
 W_2 = & -\frac{1}{3F_d^4} \left[f_1^2 e^{-k_0 f_1} K_0(k_0 f_1) + f_2^2 e^{-k_0 f_2} K_0(k_0 f_2) \right] \\
 & + \frac{2(f_1^2 - f_1 f_2 + f_2^2)}{3F_d^4} e^{-k_0(f_1 + f_2)/2} K_0\left(\frac{k_0(f_1 + f_2)}{2}\right) \\
 & + \frac{4}{3F_d^2} \left[\left(\frac{f_1^2}{F_d^2} + f_1 \right) e^{-k_0 f_1} K_1(k_0 f_1) + \left(\frac{f_2^2}{F_d^2} + f_2 \right) \right. \\
 & \times e^{-k_0 f_1} K_1(k_0 f_1) - \left\{ \frac{(f_1 + f_2)^2}{2F_d^2} - (f_1 + f_2) \right\} e^{-k_0(f_1 + f_2)/2} \\
 & \times \left. K_1\left(\frac{k_0(f_1 + f_2)}{2}\right) \right]
 \end{aligned}$$

The optimum value of the distance, a which makes $R_{\ell\ell 1}$ minimum is obtained numerically as in Cases I and II. The optimum values of μ_1 and μ_2 were calculated for various values of f_1 and f_2 . The results of these calculations are shown in Figures 12 and 13. The wave resistance coefficient for the obtained optimum parameters for each Froude number is also calculated, but this is the same as that of Case II.

18. EFFECT OF STERN

The stern can be represented as a uniform sink line from $(L, 0, 0)$ to $(L, 0, -1)$ whose total strength is the same as the source line. Here L is nondimensionalized with respect to d . The wave resistance due to the source and sink lines alone excluding interferences is as twice as that due to the source line alone. However, the effect of the interference between the

singularities representing the forward and aft part of the ship may be extremely important. The wave resistance between the source and sink lines R_{1i} , is evaluated using the method of stationary phase (see e.g. Stoker, 1957) in nondimensional form.

$$\begin{aligned} R_{1i} &= -4 \int_0^{\pi/2} \left(1 - e^{-k \sec^2 \theta}\right)^2 \cos \theta \cos (k_o L \sec \theta) d\theta \\ &= -2 \left(\frac{2\pi}{k_o L}\right)^{\frac{1}{2}} \left(1 - e^{-k_o}\right)^2 \cos (k_o L + \frac{\pi}{4}) \end{aligned} \quad [48]$$

which is approximately valid when $F_L = \sqrt{\frac{1}{k_o L}} < .4$ (Inui, 1955).

Similarly the wave resistance due to the interference between the doublet line and the sink line is

$$\begin{aligned} R_{2i} &= 2 \left(1 - e^{-k_o}\right) \left[\frac{1}{F_d^2} \left\{ e^{-k_o f_1} (\mu_2 f_1 + \mu_1) - e^{-k_o f_2} (\mu_2 f_2 + \mu_1) \right\} \right. \\ &\quad \left. + \mu_2 \left(e^{-k_o f_1} - e^{-k_o f_2} \right) \right] \left(\frac{2\pi}{k_o (a+L)} \right)^{\frac{1}{2}} \sin \left\{ k_o (a+L) + \frac{\pi}{4} \right\} \end{aligned} \quad [49]$$

The optimum values of μ_1 and μ_2 change very slightly when the sink line stern is considered (see Table 1).

The total resistance for the system including the sink line stern and optimum doublet lines is plotted in Figure 15 for Froude numbers, $F_L = 0.2, 0.25$, and 0.3 . The numerical values of the stern effect for each Froude number are also shown in Table 1. Here we can see that the interference between the stern and the bow plus bulb is in general much less than that of the stern and the bow alone. That is, the bulb has an effect

of smoothing out the humps and hollows of the resistance curve to a considerable extent. Besides, the magnitude of the interference resistance between the bulb and the bow is much larger than either the interference resistance between the stern and the bow or between the stern and the bulb.

19. DISCUSSION

Under the optimum conditions, the effect of the line doublet is similar to that of the point doublet of equal total strength. The optimum position of the center of gravity of the line doublet increases in depth and moves forward with increasing Froude number while at the same time increasing in total strength. This is shown by Table 1, Figures 12 and 13. The total effect of the line doublet on the wave resistance is almost exactly the same as that of the point doublet.

The wave resistance curves due to the systems of source line and the doublet line alone optimized for Froude numbers $F_L = 0.2, 0.25$, and 0.3 are shown in Figure 14. The wave resistance at a little lower Froude numbers than the optimum Froude numbers is larger than that due to the source line alone, but at Froude numbers in the vicinity of and greater than that for which the line doublet was optimized, the effect of the line doublet (bulb) is always to reduce the wave resistance.

The variation of the strength of the doublet line (assumed to be linear) is very small in general unless we make the doublet line long enough so that its upper end is very near to the free surface. In this case the optimum slope is quite large for low Froude numbers. However, the upper end of the linear doublet line should not be too close to the free surface for optimum interference. In fact, it can be seen from Table 1 that

the optimum depth of the upper end increases with increasing Froude number.

20. APPLICATION

If we want to improve the ship shape of length L , whose waterline is given by the polynomial (G. P. Weinblum, 1950) as

$$\sum_{n=0}^{5} \frac{A_n}{n+1} x^{n+1}$$

then the singularity distribution in the sense of Michell's ship is

$$\sum_{n=0}^{5} A_n x^n$$

The height of bow wave at a large x is given by (see Equations [25], [26]),

$$\begin{aligned} \zeta_{bs} = & \frac{8}{V k_o} \int_0^{\pi/2} \left(1 - e^{-k_o z_1 \sec^2 \theta} \right) \left\{ a_o - \frac{2! a_2}{k_o^2 \sec^2 \theta} + \frac{4! a_4}{k_o^4 \sec^4 \theta} \right. \\ & \times \sin(k_o x \sec \theta) + \left[-\frac{a_1}{k_o \sec \theta} + \frac{3! a_3}{k_o^3 \sec^3 \theta} - \frac{5! a_5}{k_o^5 \sec^5 \theta} \right] \cos(k_o x \sec \theta) \Big\} \\ & \times \cos(k_o y \sin \theta \sec^2 \theta) d\theta \end{aligned} \quad [50]$$

If we combine the bulb whose wave height at a large x is

$$\begin{aligned} \zeta_b = & -\frac{8k_o^2 \mu}{V} \int_0^{\pi/2} \sec^4 \theta e^{-k_o f \sec^2 \theta} \left\{ \sin(k_o x \sec \theta) \cos(k_o a \sec \theta) \right. \\ & \left. + \cos(k_o x \sec \theta) \sin(k_o a \sec \theta) \cos(k_o y \sin \theta \sec^2 \theta) \right\} d\theta \end{aligned}$$

the wave resistance due to this bulb and bow are obtained from

Equation [29] and are given by

$$\begin{aligned}
 R = 16\rho\pi \int_0^{\pi/2} & \left[\left[1 - e^{-k_0 z \sec^2 \theta} \right] \left(\frac{a_0}{k_0} - \frac{a_1 a_2}{k_0^3 \sec^2 \theta} + \frac{4! a_4}{k_0^5 \sec^4 \theta} \right) \right. \\
 & - \mu k_0^2 e^{-k_0 f \sec^2 \theta} \sec^4 \theta \cos (k_0 a \sec \theta) \left. \right]^2 \cos^3 \theta \\
 & + \cos^3 \theta \left[1 - \left(e^{-k_0 z \sec^2 \theta} \right) \left(- \frac{a_1}{k_0^2 \sec \theta} + \frac{3! a_3}{k_0^3 \sec^3 \theta} - \frac{5! a_5}{k_0^5 \sec^5 \theta} \right) \right. \\
 & \left. - \mu k_0^2 e^{-k_0 f \sec^2 \theta} \sec^4 \theta \sin (k_0 a \sec \theta) \right]^2 d\theta .
 \end{aligned}$$

All the integrals involved here are of the form

$$I_n = \int_0^{\pi/2} e^{-2h \sec^2 \theta} \sec^{2n+1} \theta d\theta \quad (\text{shown in Equation [14]})$$

if we consider the expansion of $\cos (k_0 a \sec \theta)$ and $\sin (k_0 a \sec \theta)$.

Hence the wave resistance in this case may be evaluated exactly in the same manner as in Section 5.

The optimum parameters, f , μ , and a may be determined by the methods used in Sections 7 and 12.

If we include the stern the expression for the wave resistance becomes a little complicated. However, the forms of the integrals are the same as those encountered previously when the method of stationary phase was used for $F < 0.4$.

Since the effect of the bulb is largely due to the interference of the bulb with the bow wave (Takahei, 1960), we need not be concerned about the influence of the stern in dealing with the determination of the optimum bulb parameters even though they vary slightly as shown in Section 18.

The elementary bow waves (Havelock, 1934a) of usual ships are combinations of sine waves and cosine waves as shown in Equation [50]. Since the best position of the doublet for the sine bow waves can be easily shown to be at the bow itself, the distance between the doublet and the bow in the case of usual ships will not be as large as is in the case of a source line ship. Hence the series expansion used in finding the distance may be evaluated more easily.

APPENDIX

Consider

$$R_i(t, h, 2v) = \int_0^{\pi/2} e^{-2h \sec^2 \theta} \sec^{2v} \theta \sin(t \sec \theta) d\theta.$$

Expanding $\sin(t \sec \theta)$ we have for the integrand

$$\sum_{n=0}^m \frac{(-1)^n (t \sec \theta)^{2n+1}}{(2n+1)!} e^{-2h \sec^2 \theta} \sec^{2v} \theta + R_m,$$

where R_m is the remainder and $|R_m| \leq \frac{(t \sec \theta)^{2m+3}}{(2m+3)!} e^{-2h \sec^2 \theta} \sec^{2v} \theta$ [A1]

in $0 \leq \theta \leq \pi/2$ by Taylor's remainder theorem. It then follows that

$$R_i(t, h, 2v) = \frac{e^{-h}}{2} \sum_{n=0}^m \frac{t^{2n+1}}{(2n+1)! 2^{n+v}} \left\{ K_o(h) - K_o'(h) \right\}_{(n+v)} + \int_0^{\pi/2} R_m d\theta.$$

To prove

$$R_i(t, h, 2v) = \frac{e^{-h}}{2} \sum_{n=0}^{\infty} \frac{t^{2n+1}}{(2n+1)! 2^{n+v}} \left\{ K_o(h) - K_o'(h) \right\}_{(n+v)}$$

we have only to prove

$$\lim_{m \rightarrow \infty} \int_0^{\pi/2} R_m d\theta = 0.$$

By the inequality [A1],

$$\begin{aligned} \left| \int_0^{\pi/2} R_m d\theta \right| &\leq \int_0^{\pi/2} e^{-2h \sec^2 \theta} \frac{t^{2m+3} \sec^{2v+2m+3} \theta}{(2m+3)!} d\theta \\ &= \frac{t^{2m+3} \left\{ K_o(h) - K_o'(h) \right\}_{(m+1+v)}}{(2m+3)! 2^{m+1+v}} \end{aligned}$$

Next, for later use we have to prove an inequality

$$K_v(h) \leq \frac{2^{v-1}}{h^{v-1}} \quad v! \quad K_1(h) \quad [A2]$$

where $0 < h < 1$ and v is a positive integer.

From the recurrence formulae

$$K_{v+1}(h) = \frac{2^v}{h} K_v(h) + K_{v-1}(h) \quad [A3]$$

Suppose we have the inequality [A2] for v and $v-1$. Putting inequality [A2] into Equation [A3], we get

$$\begin{aligned} K_{v+1}(h) &\leq \frac{2^v}{h^v} v v! K_1(h) + \frac{2^{v-2}}{h^{v-2}} (v-1)! K_1(h) \\ &\leq \frac{2^v (v+1)}{h^v} ! K_1(h) \end{aligned}$$

But we know

$$K_1(h) = K_1(h)$$

$$K_2(h) \leq 2 \cdot 2 ! K_1(h)$$

Hence by the mathematical induction, the inequality [A2] is true.

From the recurrence formula

$$-K_v'(h) = \frac{1}{2} \left(K_{v-1}(h) + K_{v+1}(h) \right)$$

we can prove

$$\left. \begin{aligned} (-1)^v \frac{d^v K_0(h)}{dh^v} &\leq K_v(h) + K_{v-2}(h) + \dots + K_1(h) \text{ when } v \text{ is odd} \\ &\leq K_v(h) + K_{v-2}(h) + \dots + K_0(h) \text{ when } v \text{ is even} \end{aligned} \right\} [A4]$$

By definition

$$\begin{aligned}
 K_o(h) - K_o'(h) \Big|_{(n)} &= K_o(h) - \binom{n}{1} \frac{dK_o(h)}{dh} + \binom{n}{2} \frac{d^2K_o(h)}{dh^2} - \dots \\
 &\quad + (-1)^n \frac{d^nK_o(h)}{dh^n} \tag{A5}
 \end{aligned}$$

Using the inequalities [A2] and [A4] in Equation [A5] we can prove

$$\begin{aligned}
 \left\{ K_o(h) - K_o'(h) \right\} \Big|_{(n)} &\leq \frac{nn!2^{n-1}}{h^n} K_1(h) \text{ for } v < h \leq 1 \\
 \left| \int_0^{\pi/2} R_m \, d\theta \right| &\leq \frac{t^{2m+3}}{h^m} \frac{m \cdot m! K_1(h)}{2^{2+v} (2m+3)!}
 \end{aligned}$$

The left hand side will approach zero when m becomes larger than t^2/h . When $h > 1$ the proof is simpler.

REFERENCES

1. Eggart, E. F., "Form Resistance Experiment", SNAME, 1935.
2. Gill, S. A., "A Process for the Step-by-Step Integration of Differential Equations in an Automatic Digital Computing Machine", Proc. Cambridge Philos. Soc., Vol. 47, pp. 96-108, 1951.
3. Havelock, T. H., "The Wave Pattern of a Doublet in a Stream", Proc. Roy. Soc., A Vol. 121, p. 515-23, 1928; "Wave Patterns and Wave Resistance", T.I.N.A., Vol. 76, pp. 430-443, 1934a; "The Calculation of Wave Resistance", Proc. Roy. Soc., A Vol. 144, pp. 514-521, 1934b.
4. Inui, T., "Asymptotic Expansion Applied to Problems in Ship Waves and Wave-Making Resistance", Proc. of the 5th Japan National Congress for App. Mech., 1955.
5. Inui, T., 60th Anniversary Series, Vol. 2, 1960.
6. Inui, T., Takahei, T. and Kumano, M., "Wave Profile Measurements on the Wave-Making Characteristics of the Bulbous Bow", Society of Naval Architecture of Japan, 1960.
7. Kutta, W., "Beitrag zur näherungsweisen Integration totaler Differentialgleichungen", Z. Math. Phys., Vol. 46, pp. 435-453, 1901.
8. Lagally, M., "Berechnung der Kräfte und Momente, die strömende Flüssigkeiten auf ihre Begrenzung ausüben", Zeitschrift Für Angewandte Mathematik und Mechanik, Band 2, 1922.
9. Lamb, H., "Hydrodynamics", Dover Pub., New York, 1945.
10. Lunde, J. K., "On the Theory of Wave Resistance and Wave Profile", Skipsmodelltankens meddelelse Nr. 10, 1952.
11. Milne-Thomson, L. M., "Theoretical Hydrodynamics", 4th ed., Macmillan Company, New York, 1956.
12. Ralston, Anthony and Wilf, Herbert S., "Mathematical Methods for Digital Computers", John Wiley and Sons, Inc., New York, 1960.
13. Runge, C., "Über die numerische Auflösung von Differentialgleichungen", Math. Ann. Vol. 46, pp. 167-178, 1895.
14. Saunders, H. E., "Hydrodynamics in Ship Design", Vol. 1, pp. 368-371, 1957.

HYDRONAUTICS, Incorporated

-40-

15. Stoker, J. J., "Water Waves", Interscience Publishers, Inc., New York, 1957.
16. Takahei, T., "A Study on the Waveless Bow", SNAJ, 1960.
17. Taylor, D. W., "Some Model Basin Investigations of the Influence of Form of Ships on Their Resistances", SNAME, 1911.
18. Taylor, D. W., "The Speed and Power of Ships", 3rd ed. U. S. Gov't Printing Office, Washington, D. C., 1943.
19. Weinblum, G. P., "Die Theorie der Wulstschiffe", Der Gesellschaft für Angewandte Mathematik, 1935.
20. Weinblum, G. P., "Analysis of Wave Resistance", DTMB, Report 710, 1950.
21. Wigley, W.C.S., "The Theory of the Bulbous Bow and its Practical Application", Trans. N.E.C.I.E.S., Vol. LII, pp. 65-88, 1936.

HYDRONAUTICS, Incorporated

TABLE 1a.

OPTIMUM PARAMETERS AND THE WAVE RESISTANCE ($d/L = 0.07$)

F_L	.15	.2	.25	.3
μ_{10}	.14447	7.5706-02	9.2753-02	.24825
μ_{20}	-1.2661-04	-3.0208-03	7.2169-04	-2.9446-05
f_1	.02	.02	.02	.04
f_2	.03	.07	.07	.07
a	.0295	.048	.06875	.09792
$R_{\ell b}$	24.108	20.480	15.756	11.747
$R_{\ell s}$	30.818	26.682	21.389	16.697
$R_{\ell \ell i}$	-48.217	-40.960	-31.513	-23.493
R	6.7090	6.2019	5.6327	4.9505
R_{1i}	-3.4890	-8.7006	4.3106	-5.5123
R_{2i}	5.9074	10.170	-6.3734	2.5322
R_t	39.9452	34.353	24.959	18.667
μ_{1s}	.12678	5.7288-02	.11140	.22150
μ_{2s}	-3.0604	-1.2358-02	3.6163-03	-1.3006-04

μ_{10}, μ_{20} : Values of μ_1 and μ_2 in the negative optimum doublet strength $\mu = \mu_1 + f\mu_2$, without considering the stern.

$$7.5706-02 \equiv 7.5706 \cdot 10^{-2}$$

$R_{\ell b}, R_{\ell s}, R_{\ell \ell i}$: Wave resistance due to the doublet line, the source line, and the interference defined by Equations [45], [44], and [46] respectively

$$R = R_{\ell s} + R_{\ell b} + R_{\ell \ell i}$$

R_{1i}, R_{2i} : Wave resistance interference between the source and sink lines, and between the doublet and sink lines respectively

R_t : Total wave resistance including the stern with μ_{10} and μ_{20}

μ_{1s}, μ_{2s} : Optimum values of μ_1 and μ_2 when the stern is considered

HYDRONAUTICS, Incorporated

TABLE 1b.

OPTIMUM PARAMETERS AND THE WAVE RESISTANCE (d/L = 0.07)

F_L	.35	.4	.45	.5
μ_{10}	.28731	.32629	.36552	1.4464
μ_{20}	-1.7513-05	-2.1465-05	-1.7576-05	2.8336-07
f_1	.04	.04	.04	.06
f_2	.07	.07	.07	.07
a	.1145	.127	.1405	.15
R_{lb}	8.4268	6.5796	5.0410	3.9724
R_{ls}	13.043	10.311	8.2791	6.7546
R_{lli}	-16.853	-13.159	-10.082	-7.9447
R	4.2683	3.7315	3.2381	2.7823
R_{1i}	4.7276	-2.9417	-2.6130	-1.17448
R_{2i}	-1.8833	2.9071	.26984	-1.0252
R_t	20.160	14.008	9.1740	8.3372
μ_{1s}	.31814	.25420	.35574	1.6330
μ_{2s}	3.8745-05	-9.3216-05	-2.3353-05	7.9889-07

μ_{10}, μ_{20} : Values of μ_1 and μ_2 in the negative optimum doublet strength $\mu = \mu_1 + f\mu_2$, without considering the stern.
 $7.5706 \cdot 02 \equiv 7.5706 \cdot 10^{-2}$

R_{lb}, R_{ls}, R_{lli} : Wave resistance due to the doublet line, the source line, and the interference defined by Equations [45], [44], and [46] respectively

$$R = R_{ls} + R_{lb} + R_{lli}$$

R_{1i}, R_{2i} : Wave resistance interference between the source and sink lines, and between the doublet and sink lines respectively

R_t : Total wave resistance including the stern with μ_{10} and μ_{20}

μ_{1s}, μ_{2s} : Optimum values of μ_1 and μ_2 when the stern is considered

HYDRONAUTICS, INCORPORATED

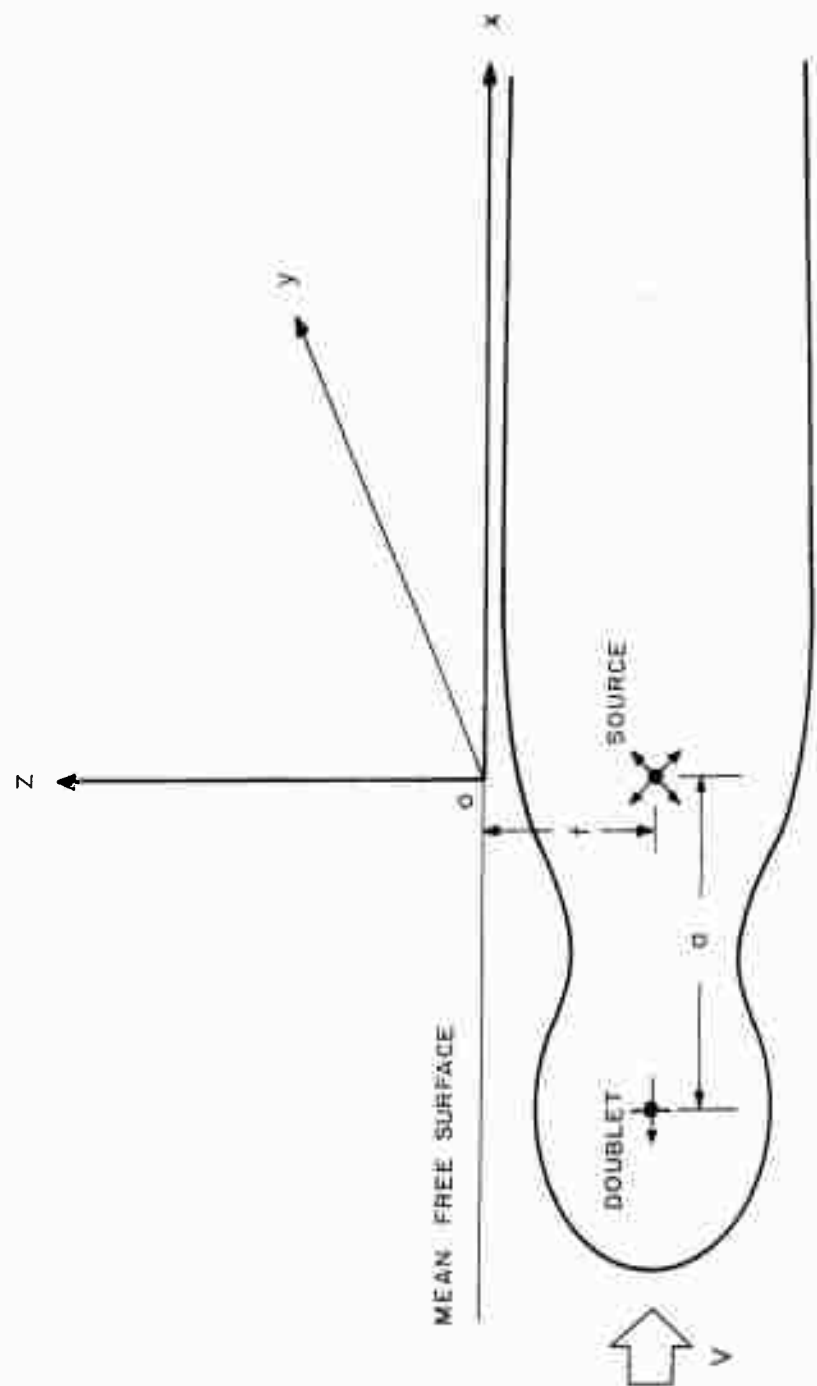


FIGURE 1- COORDINATE

HYDRONAUTICS, INCORPORATED

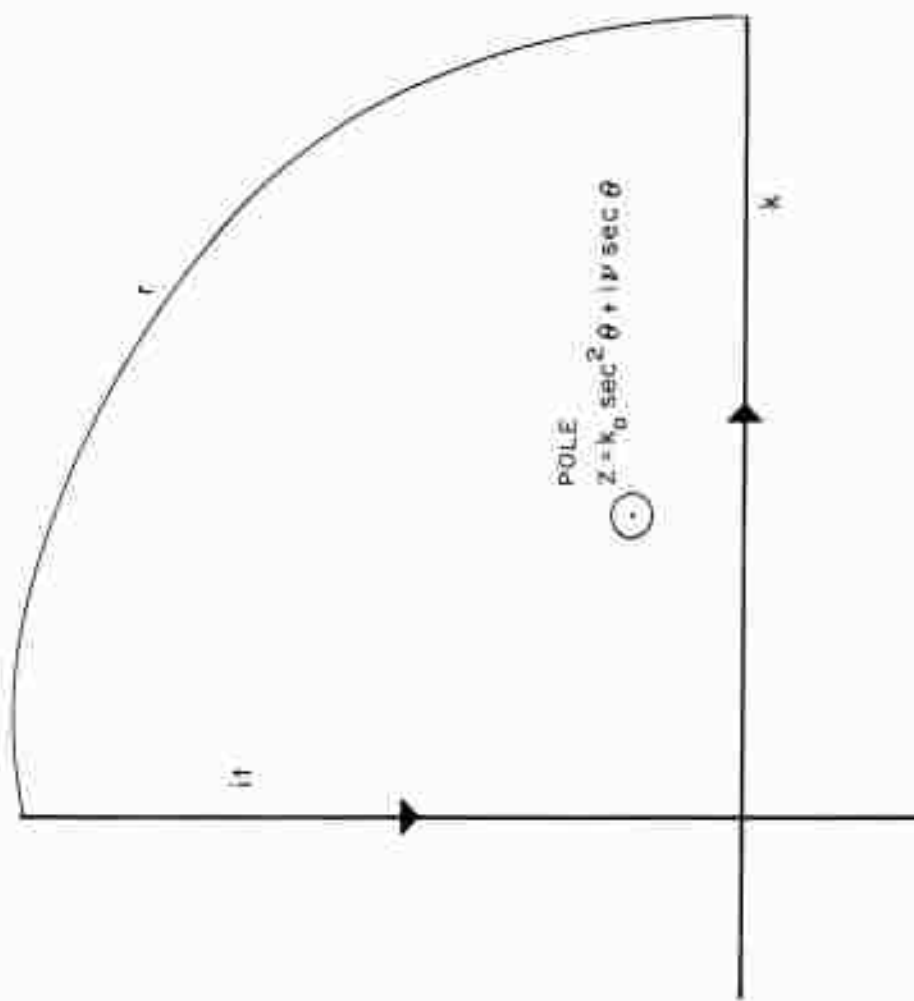


FIGURE 2- CONTOUR OF INTEGRATION

HYDRONAUTICS, INCORPORATED

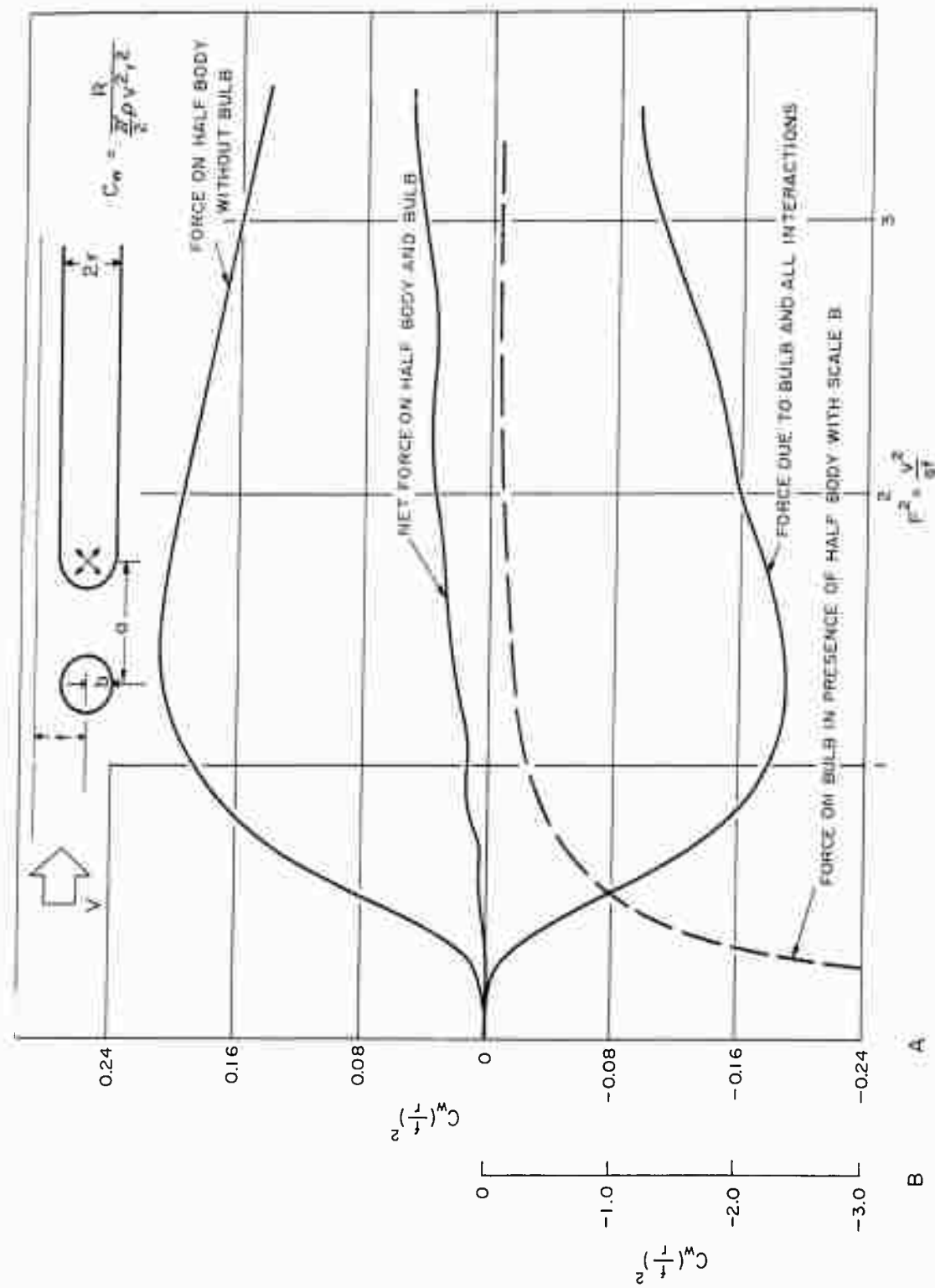


FIGURE 3 - WAVE RESISTANCE OF HALF BODY WITH OPTIMIZED BULB

HYDRONAUTICS, INCORPORATED

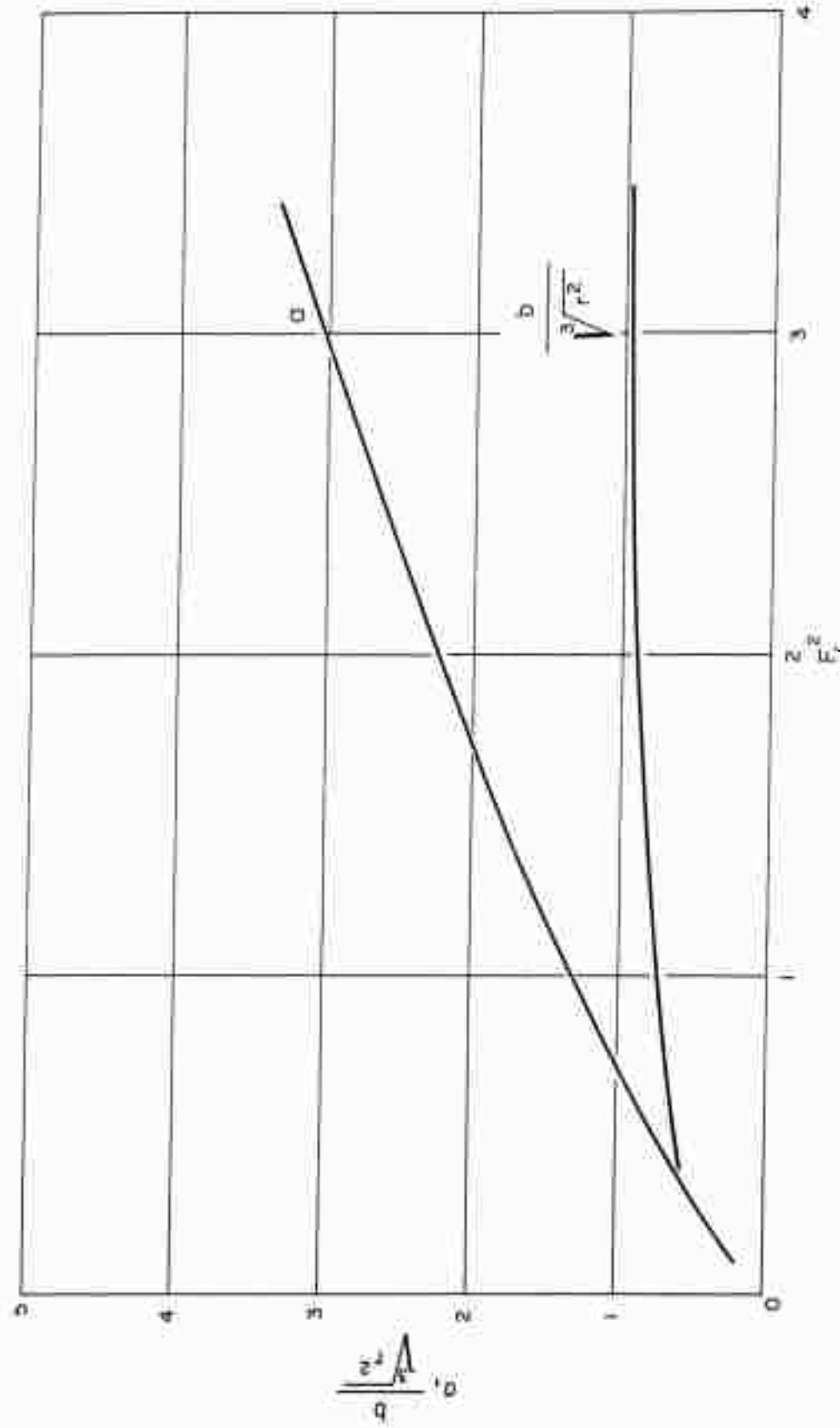


FIGURE 4 - OPTIMUM DISTANCE BETWEEN SOURCE AND DOUBLET, OPTIMUM RADIUS OF BULB
a, b, r Are Non-Dimensionalized With Respect To The Depth f

HYDRONAUTICS, INCORPORATED

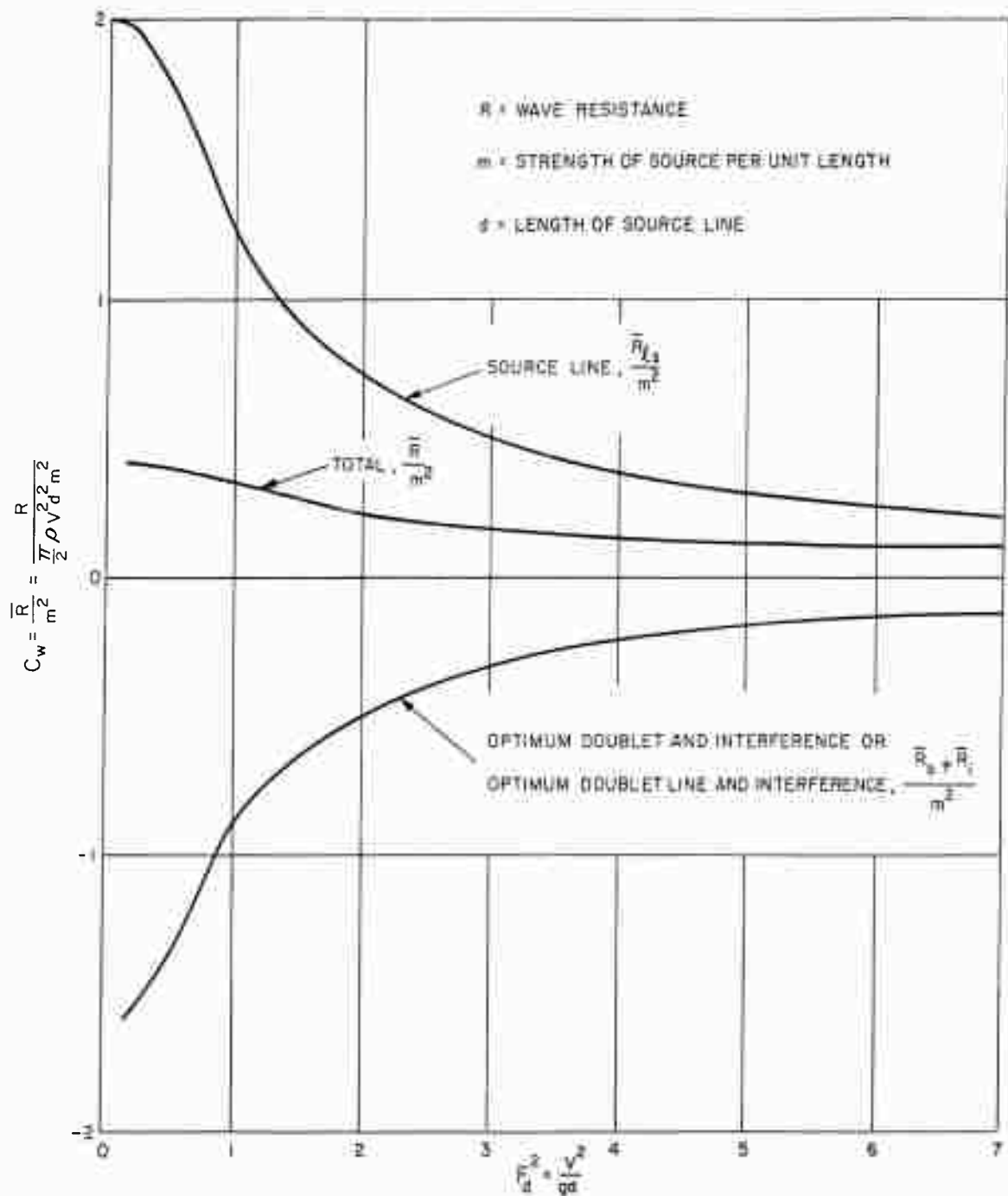


FIGURE 5- WAVE RESISTANCE OF A SOURCE LINE AND OPTIMUM DOUBLET LINE AT EACH FROUDE NUMBER

HYDRONAUTICS, INCORPORATED

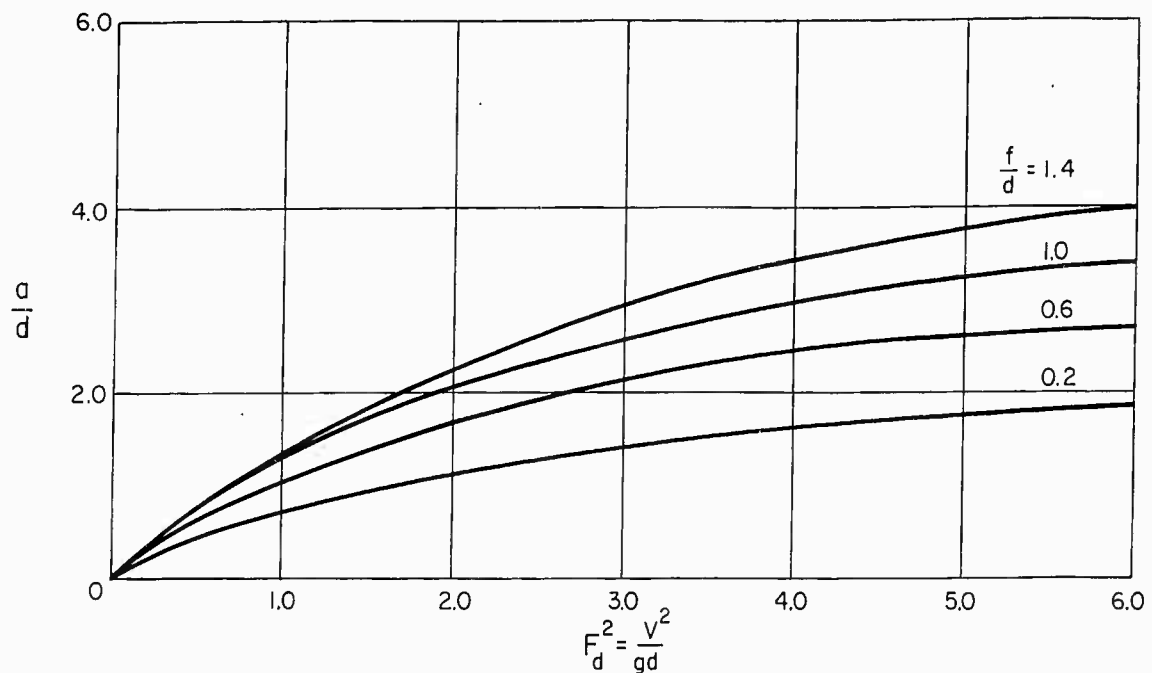


FIGURE 6- OPTIMUM DISTANCE BETWEEN DOUBLET AND SOURCE LINE

A Point Doublet At $x = -a$, $y = 0$, $z = -f$

A Source Line At $x = 0$, $y = 0$, $-d < z < 0$

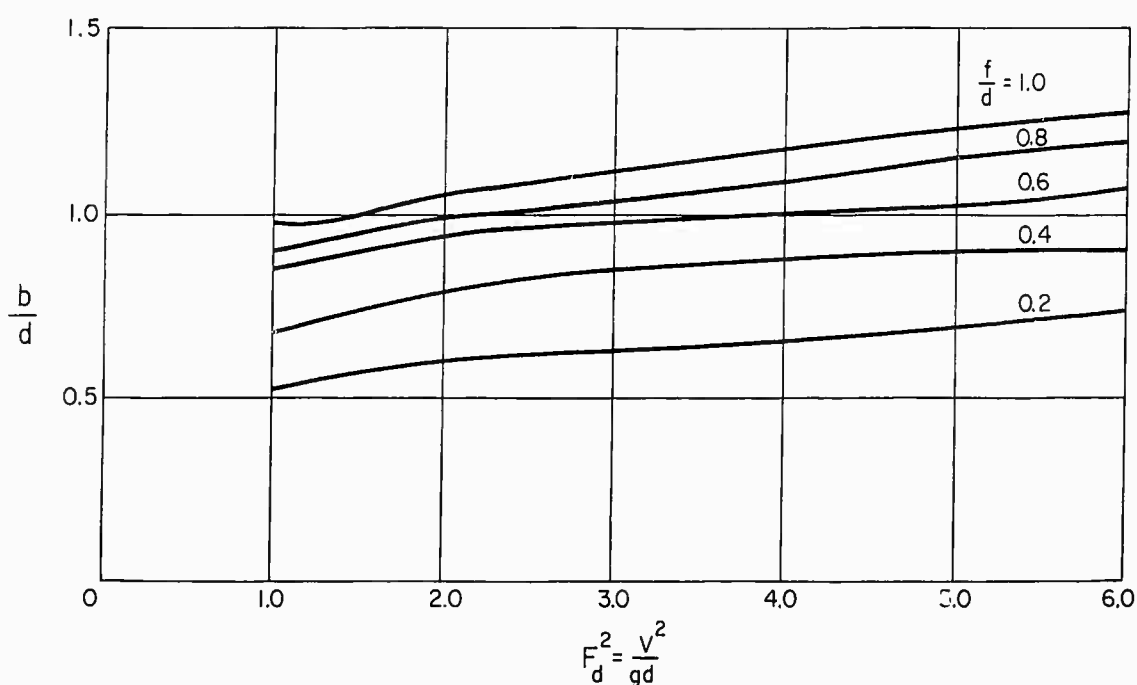


FIGURE 7- OPTIMUM RADIUS OF BULB (A POINT DOUBLET)

A Point Doublet At $x = a$, $y = 0$, $z = -f$

A Source Line At $x = 0$, $y = 0$, $-d < z < 0$

HYDRONAUTICS, INCORPORATED

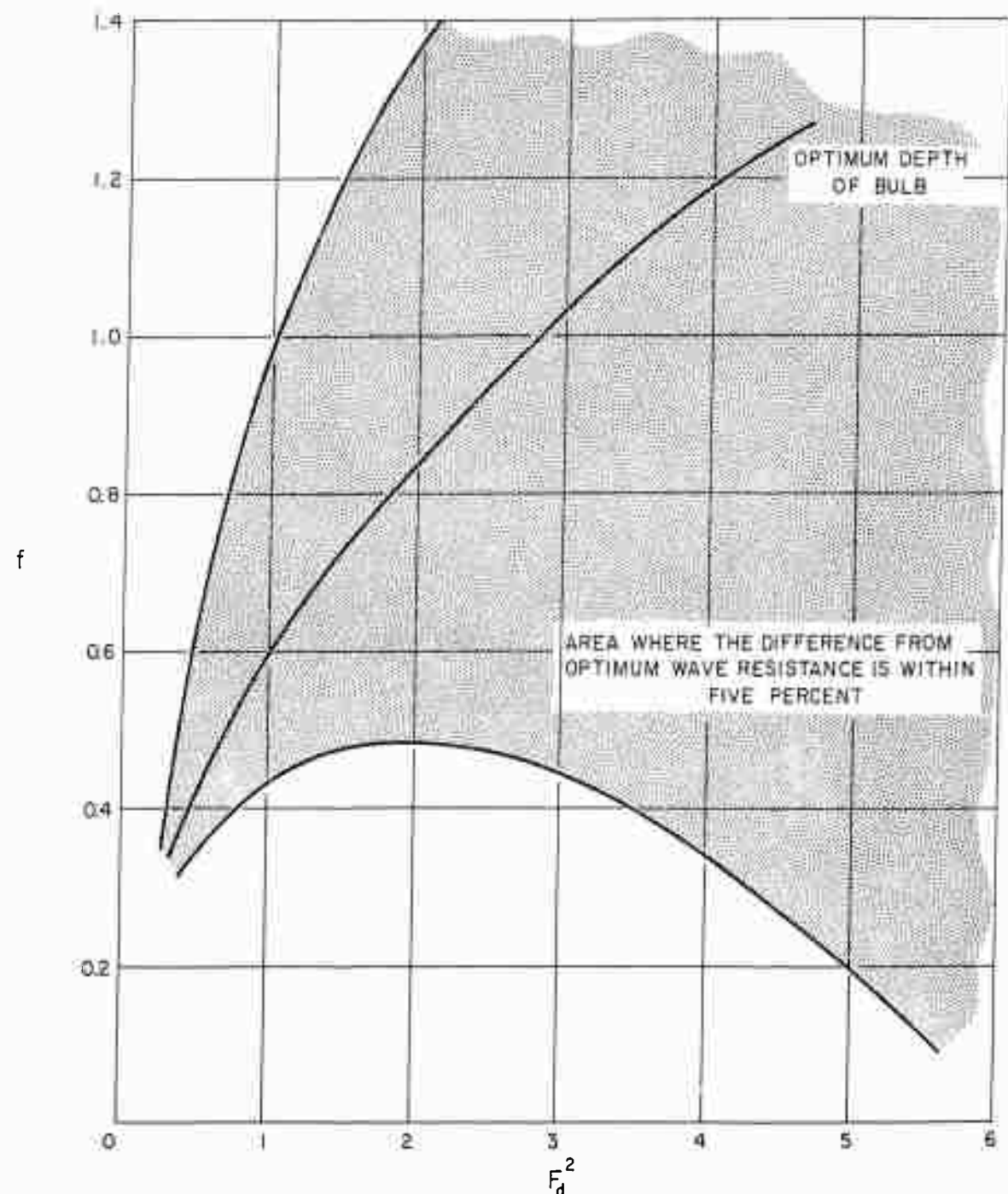


FIGURE 8 - OPTIMUM DEPTH OF DOUBLET

HYDRONAUTICS, INCORPORATED

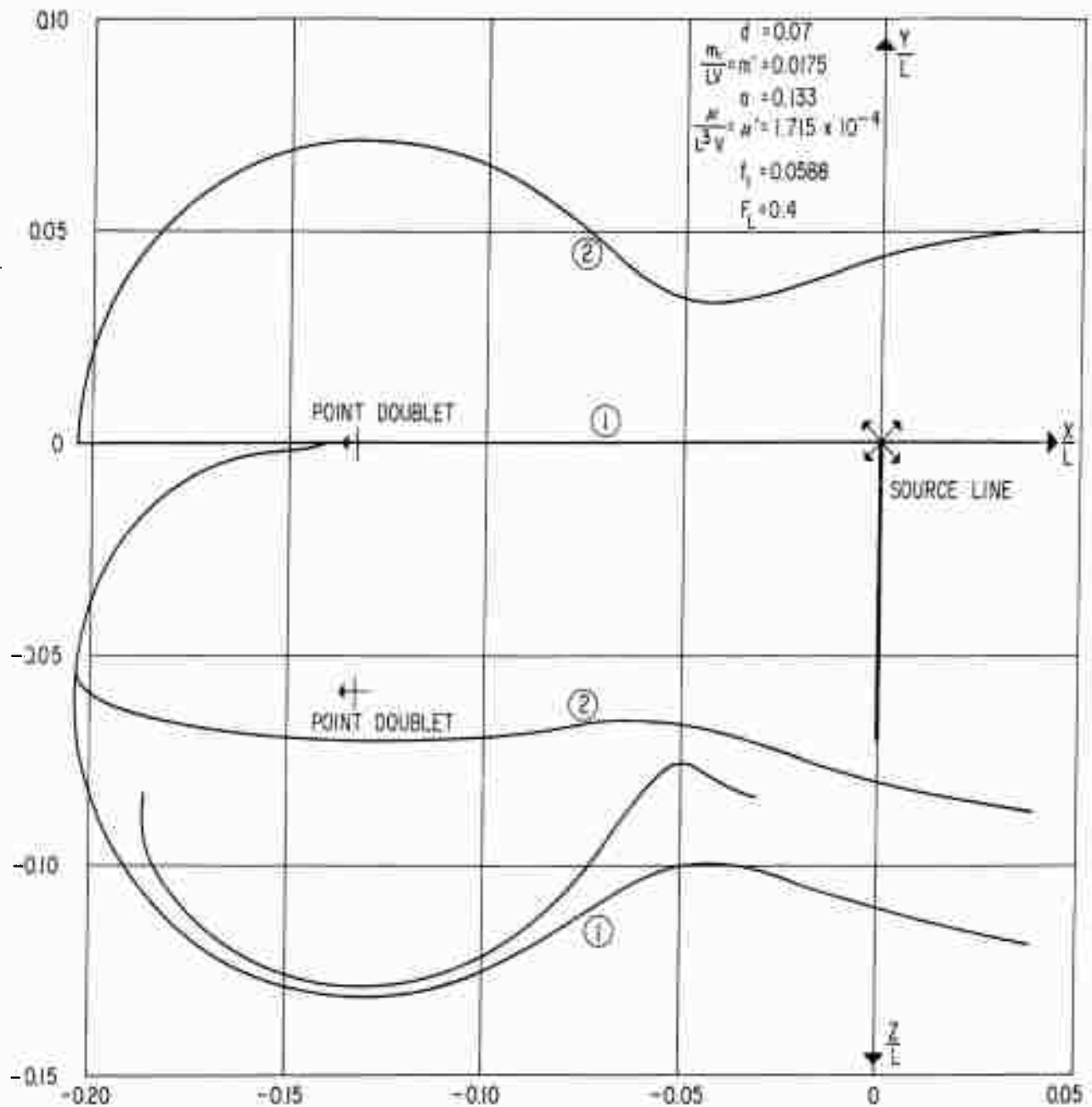


FIGURE 9- BODY STREAM-LINE SHAPE DUE TO A SOURCE LINE AND A POINT DOUBLET

HYDRONAUTICS, INCORPORATED

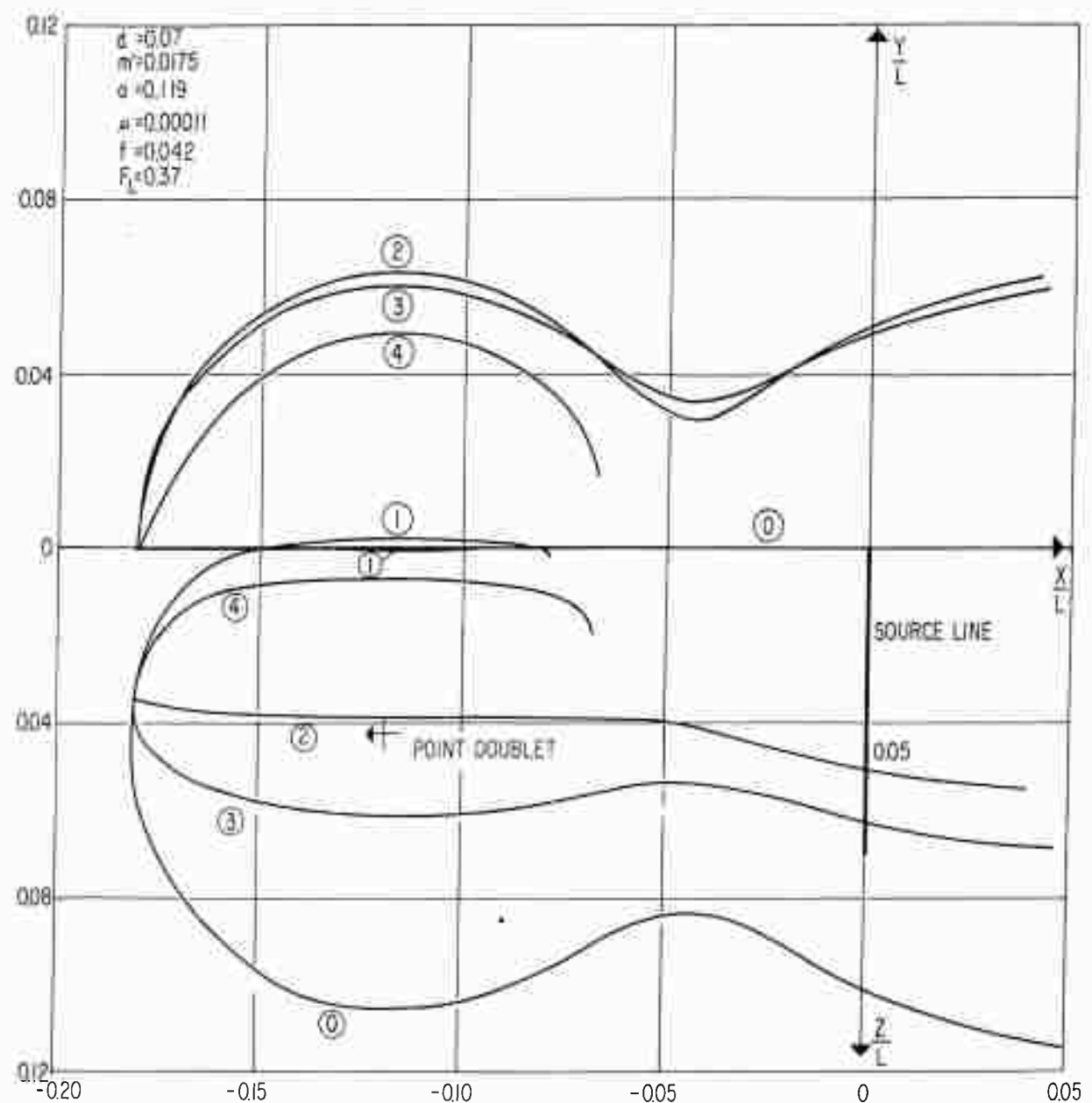


FIGURE 10 - BODY STREAM-LINE SHAPE DUE TO A SOURCE LINE AND A POINT DOUBLET

HYDRONAUTICS, INCORPORATED

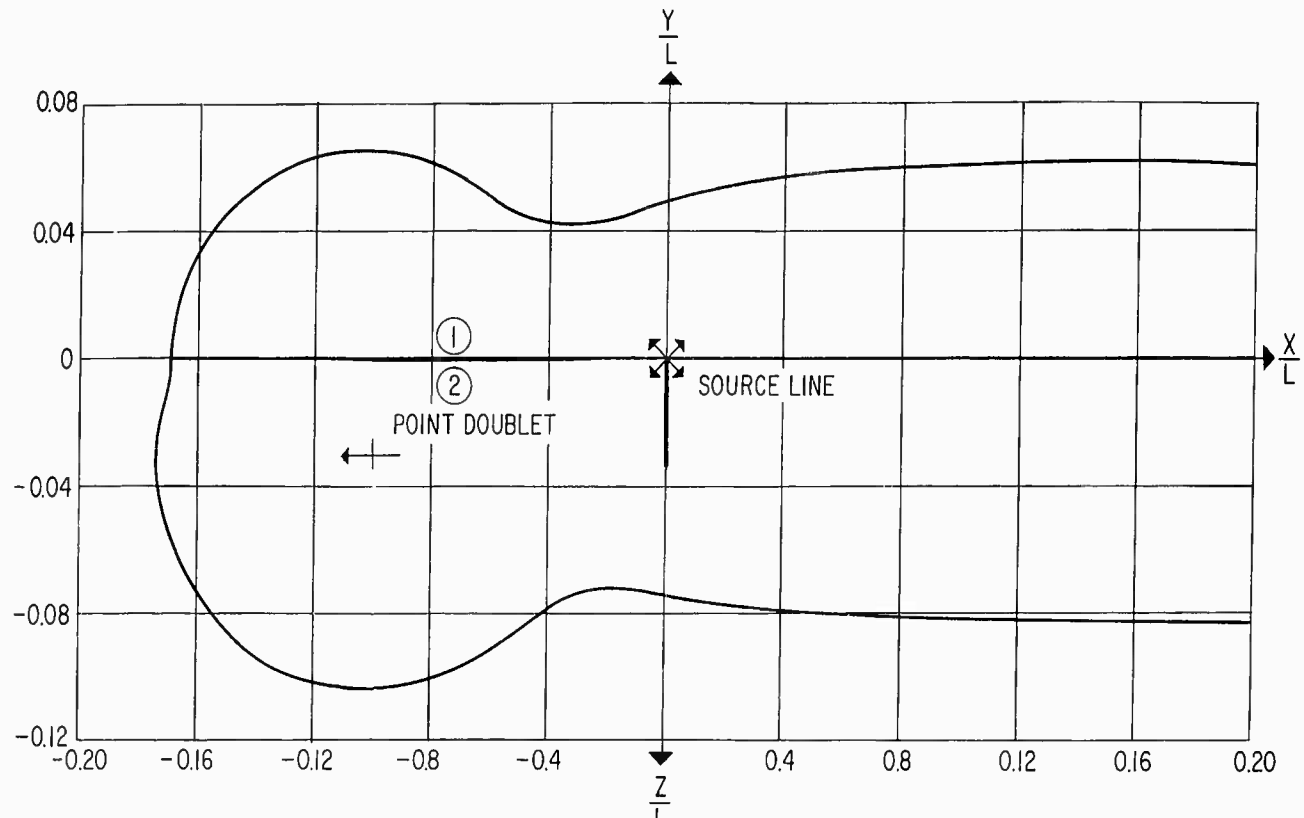


FIGURE II A

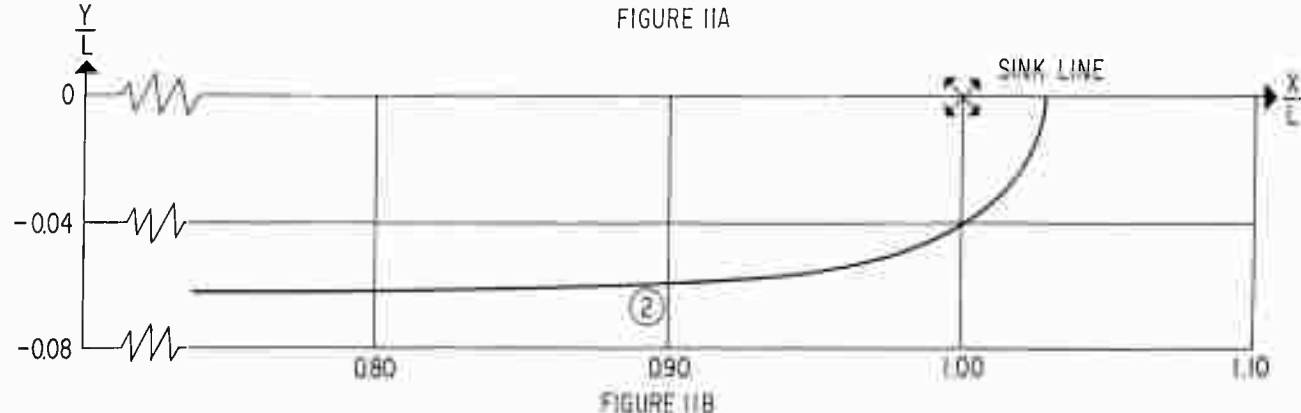


FIGURE II B

FIGURE II- BODY STREAM-LINE SHAPE OF SOURCE AND SINK LINES AND A POINT DOUBLET

$$d = 0.035 \quad \mu' = 1.42772 \times 10^{-4}$$

$$m' = 0.0175 \quad F_L = 0.37$$

$$a = 0.10395 \quad f = 0.03$$

HYDRONAUTICS, INCORPORATED

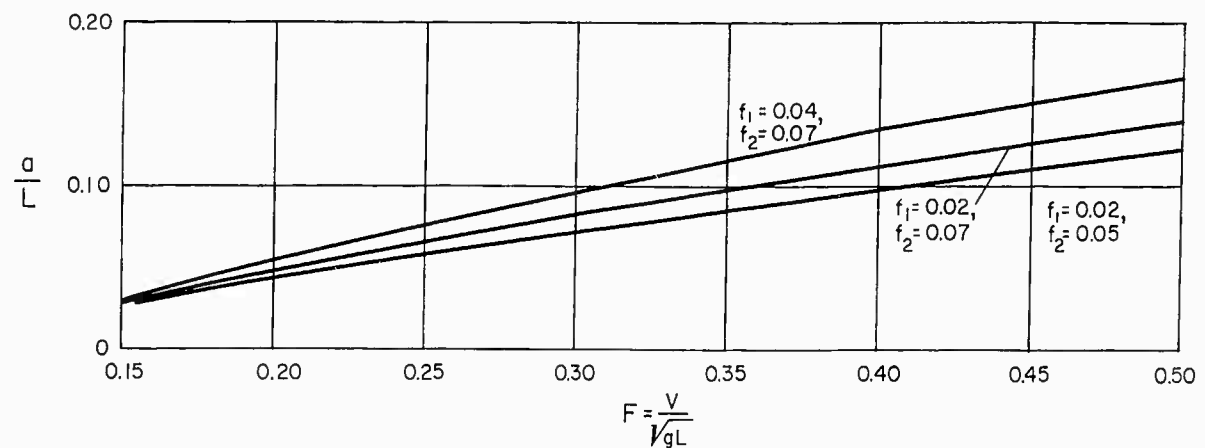


FIGURE 12 - OPTIMUM DISTANCE a , BETWEEN DOUBLET LINE AND SOURCE LINE

Doublet Line At $x=a$, $y=0$, $-f_2 < z < -f_1$, $\frac{d}{L} = 0.07$, $L = 1.0$

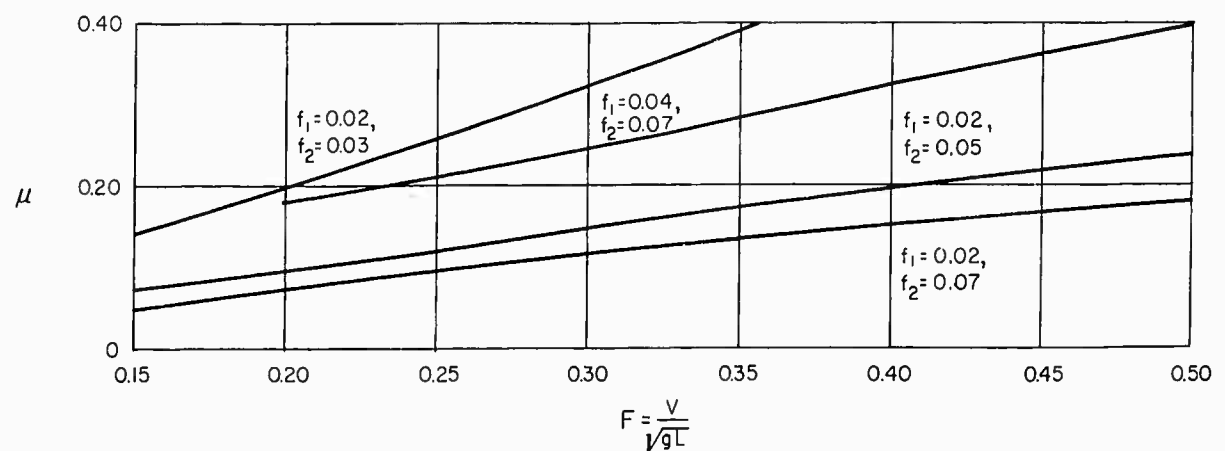


FIGURE 13 - OPTIMUM STRENGTH OF DOUBLET LINE $\mu = \mu_1 - z\mu_2$

Doublet Line At $x=a$, $y=0$, $-f_2 < z < -f_1$, $\frac{d}{L} = 0.07$, $L = 1.0$

μ_2 is Extremely Small As Shown In Table I, $x=a$ is Shown In Figure 12

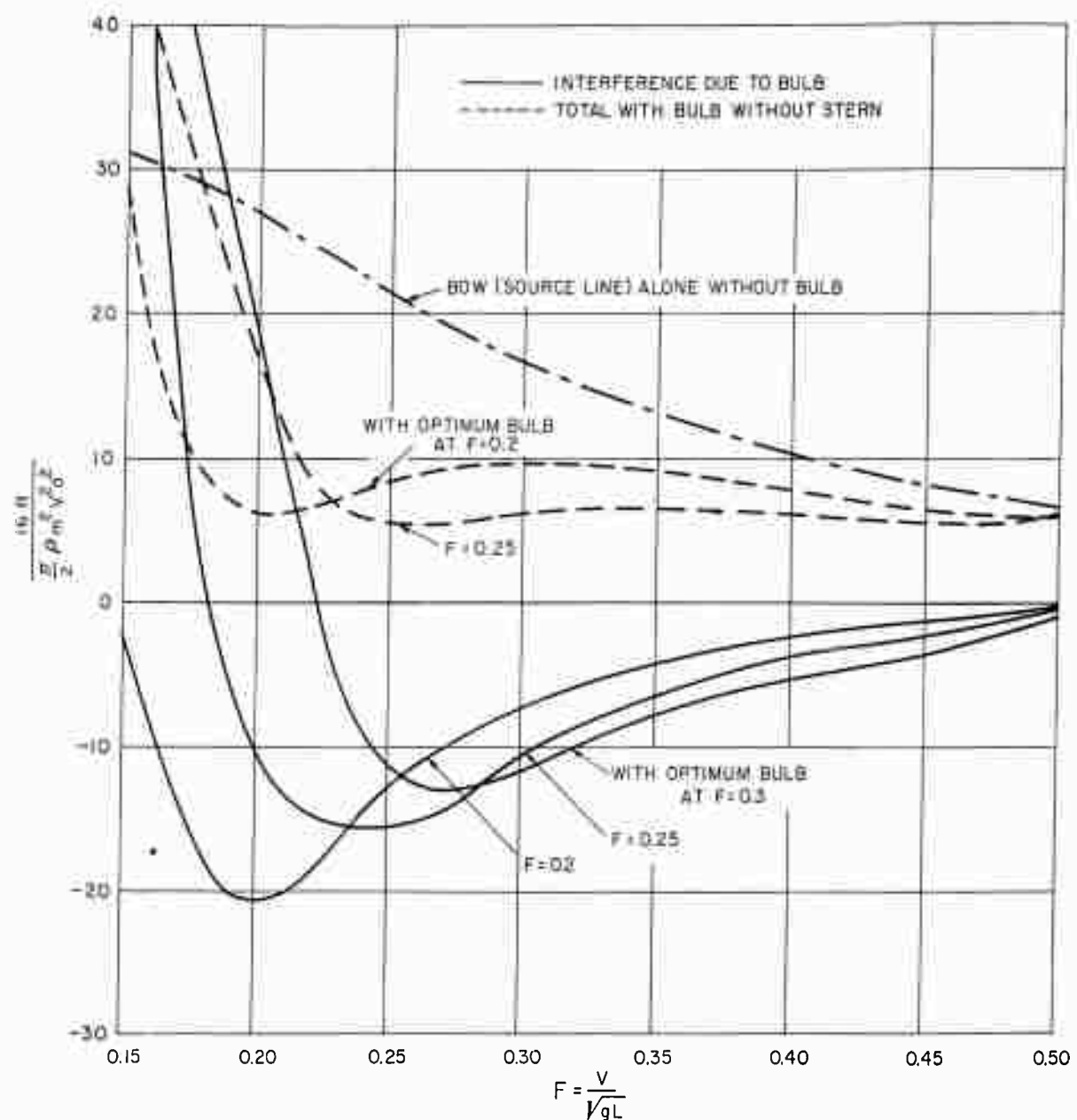


FIGURE 14 - WAVE RESISTANCE OF SOURCE LINE AND DOUBLET LINE (BULB)

Doublet Line At $x = -a, y = 0, -f_2 < z - f_1$ With Strength $\mu = \mu_1 - \mu_2 z, \frac{d}{L} = 0.07, L = 1.0$

$F = 0.20$ (Optimum)

$\mu_1 = 0.0757$

$\mu_2 = -3.026 \cdot 10^{-3}$

$f_1 = 0.02, f_2 = 0.07$

$a = 0.048$

$F = 0.25$

$\mu_1 = 0.0927$

$\mu_2 = 7.2169 \cdot 10^{-4}$

$f_1 = 0.02, f_2 = 0.07$

$a = 0.06875$

$F = 0.30$

$\mu_1 = 0.2482$

$\mu_2 = -2.9446 \cdot 10^{-5}$

$f_1 = 0.04, f_2 = 0.07$

$a = 0.0979$

HYDRONAUTICS, INCORPORATED

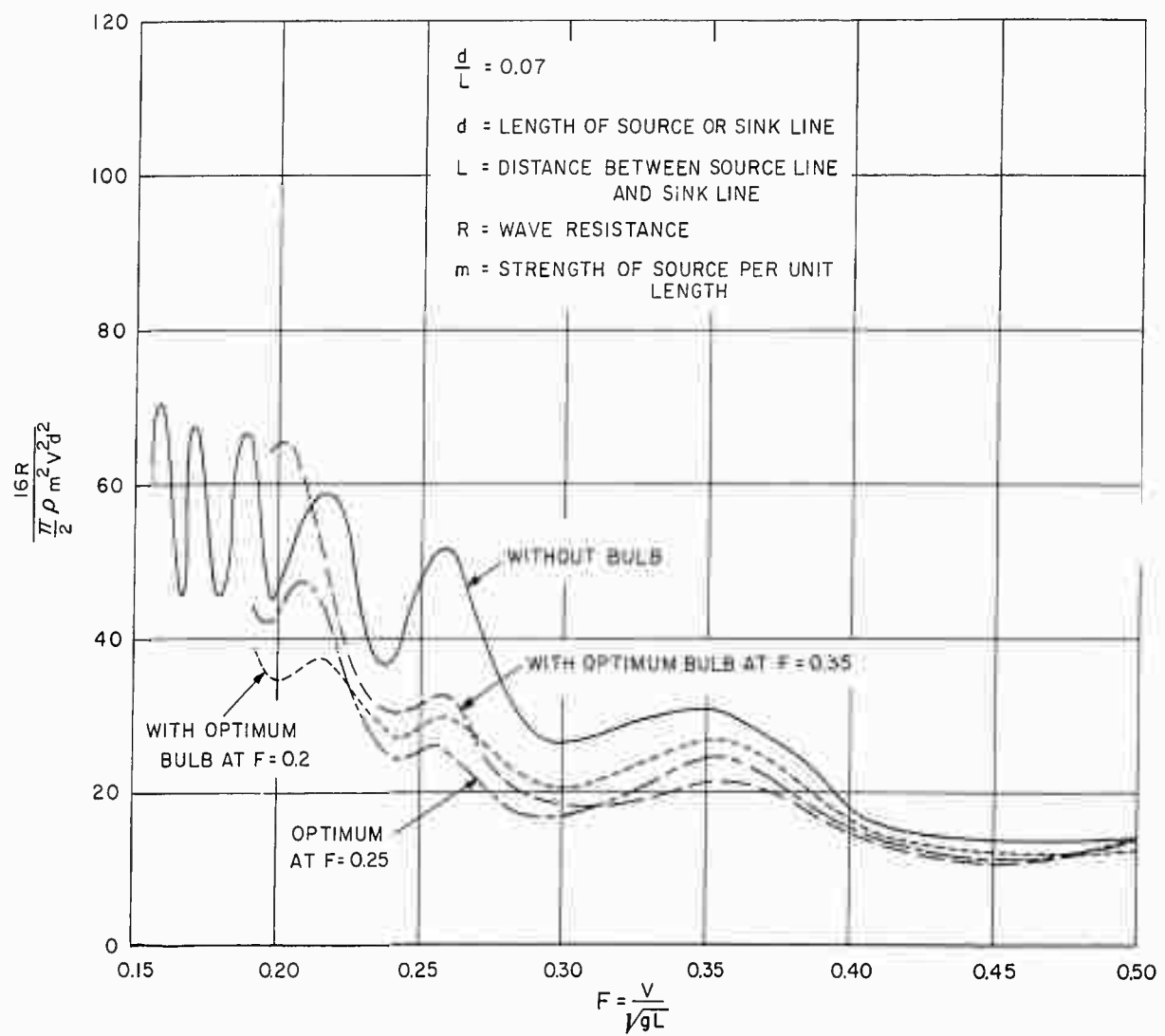


FIGURE 15 - WAVE RESISTANCE FOR SOURCE LINE SHIP INCLUDING STERN
(Sink Line)

HYDRONAUTICS, INCORPORATED

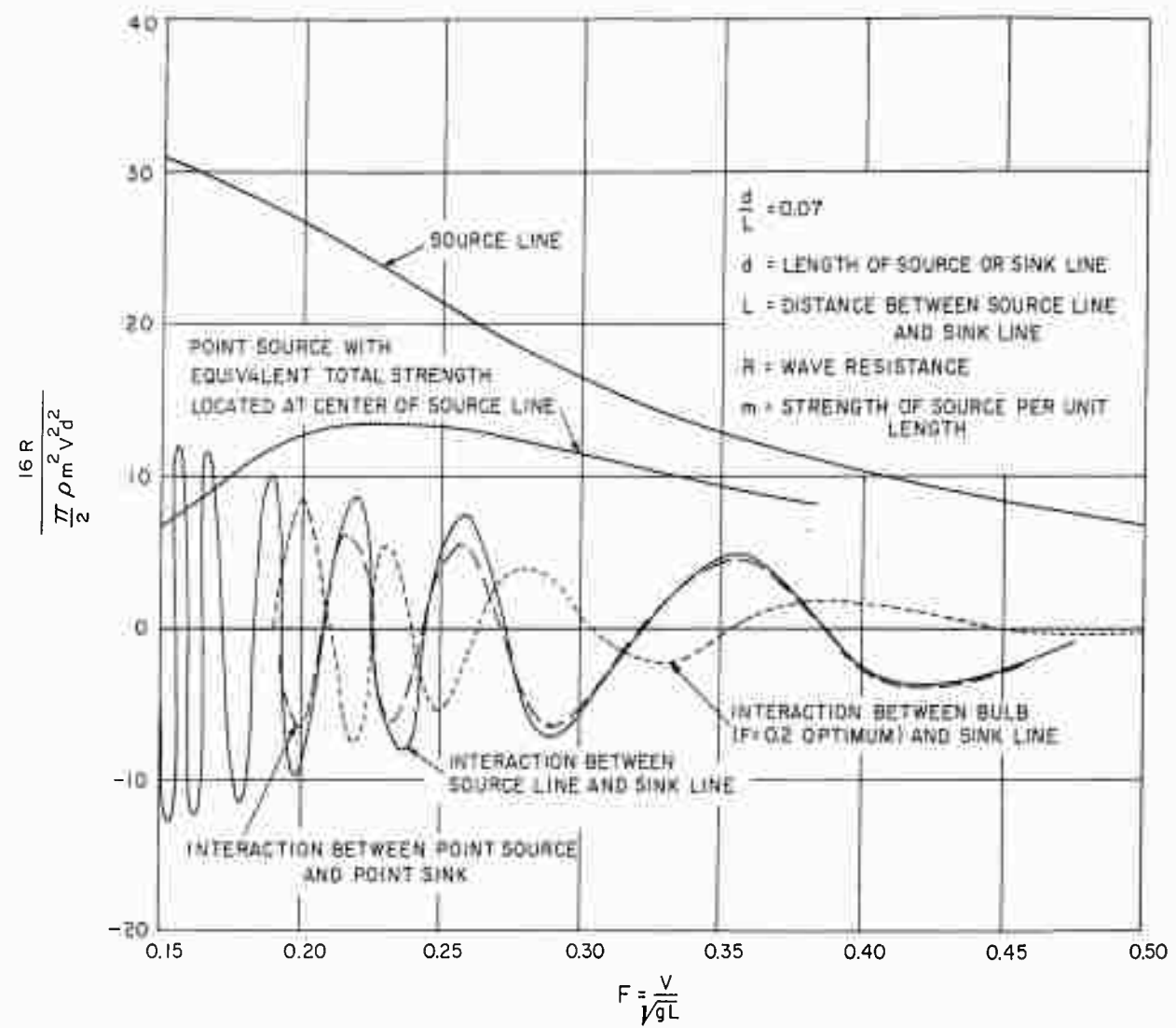


FIGURE 16 - WAVE RESISTANCE INTERFERENCE WITH STERN (Sink Line)

HYDRONAUTICS, INCORPORATED

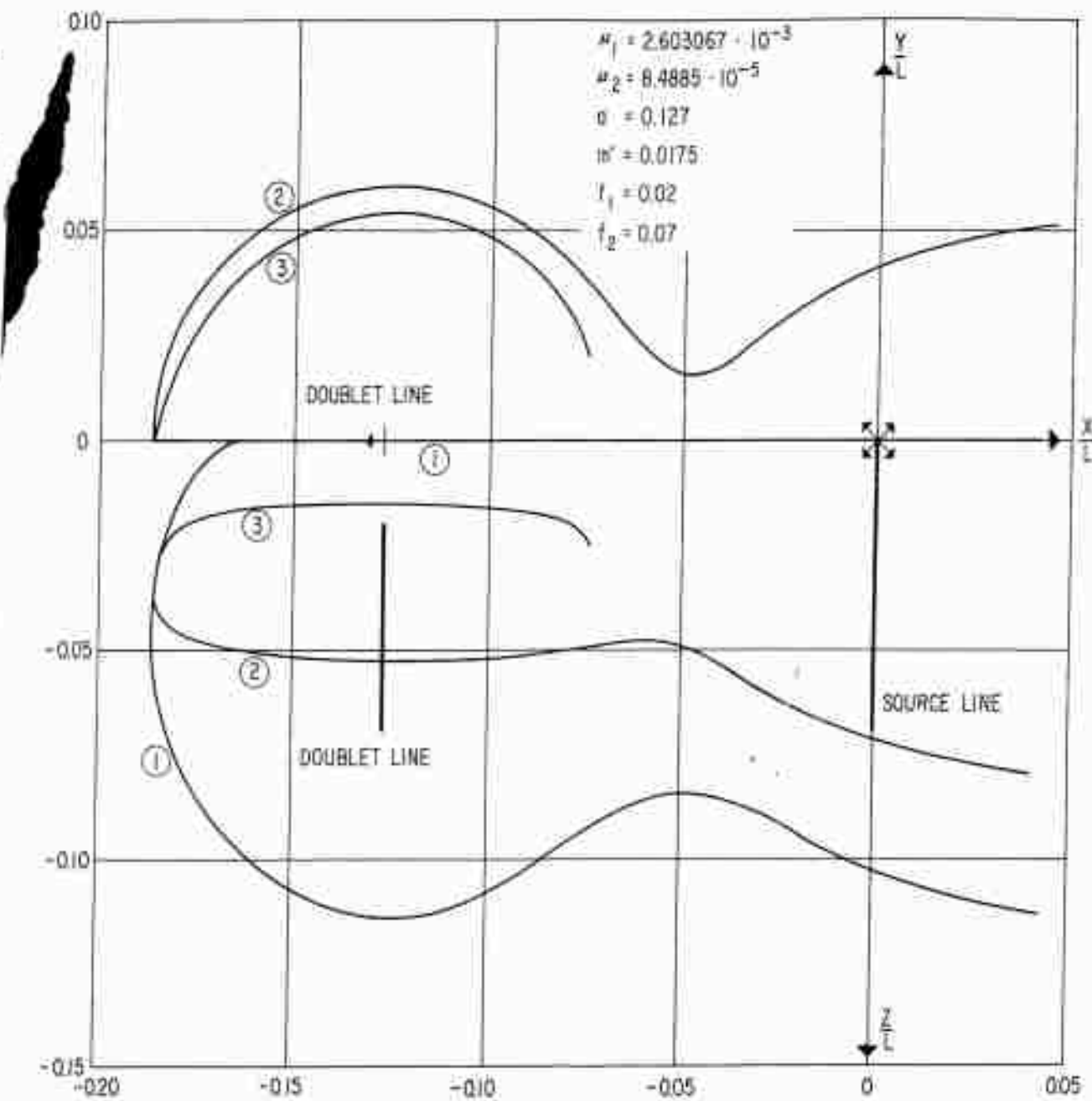


FIGURE 17- BODY STREAM-LINE SHAPE DUE TO A DOUBLET LINE AND A SOURCE LINE

Strength Of Doublet $\mu = \mu_1 - \mu_2 z$, At $x=a$, $y=0$, $-f_2 < z < -f_1$, $L=1.0$, $\frac{d}{L}=0.07$

HYDRONAUTICS, Incorporated

-i-

DISTRIBUTION LIST

Contract Nonr-3349(00)
Task NR 062-266

Chief of Naval Research Department of the Navy Washington 25, D. C. ATTN: Codes 438	3	Chief, Bureau of Ships Department of the Navy Washington 25, D. C. ATTN: Codes 106	1
461	1	310	1
463	1	312	1
466	1	335	1
		420	1
Commanding Officer Office of Naval Research Branch Office 495 Summer Street Boston 10, Massachusetts	1	421	1
		440	1
		442	1
		449	1
Commanding Officer Office of Naval Research Branch Office 346 Broadway New York 13, New York	1	Chief, Bureau of Yards and Docks Department of the Navy Washington 25, D. C. ATTN: Code D-400	1
Commanding Officer Office of Naval Research Branch Office 1030 East Green Street Pasadena, California	1	Commanding Officer and Director David Taylor Model Basin Washington 7, D. C. ATTN: Codes 108	1
		142	1
		500	1
		513	1
		520	1
		526	1
		526A	1
		530	1
		533	1
		580	1
		585	1
		589	1
		591	1
		591A	1
		700	1
Director Naval Research Laboratory Washington 25, D. C. ATTN: Code 2027	6	Commander U. S. Naval Ordnance Test Station China Lake, California ATTN: Code 753	1

HYDRONAUTICS, Incorporated

-ii-

DISTRIBUTION LIST

Commander U. S. Naval Ordnance Test Station Pasadena Annex 3202 E. Foothill Blvd. Pasadena 8, California ATTN: Code P-508	Commander Planning Department Norfolk Naval Shipyard Portsmouth, Virginia	1
Commander Planning Department Portsmouth Naval Shipyard Portsmouth, New Hampshire	Commander Planning Department Charleston Naval Shipyard U. S. Naval Base Charleston, South Carolina	1
Commander Planning Department Boston Naval Shipyard Boston 29, Massachusetts	Commander Planning Department Long Beach Naval Shipyard Long Beach 2, California	1
Commander Planning Department Pearl Harbor Naval Shipyard Navy No. 128, Fleet Post Office San Francisco, California	Commander Planning Department U. S. Naval Weapons Laboratory Dahlgren, Virginia	1
Commander Planning Department San Francisco Naval Shipyard San Francisco 24, California	Commander U. S. Naval Ordnance Laboratory White Oak, Maryland	1
Commander Planning Department Mare Island Naval Shipyard Vallejo, California	Dr. A. V. Hershey Computation and Exterior Ballistics Laboratory U. S. Naval Weapons Laboratory Dahlgren, Virginia	1
Commander Planning Department New York Naval Shipyard Brooklyn 1, New York	Superintendent U. S. Naval Academy Annapolis, Maryland ATTN: Library	1
Commander Planning Department Puget Sound Naval Shipyard Bremerton, Washington	Superintendent U. S. Naval Postgraduate School Monterey, California	1
Commander Planning Department Philadelphia Naval Shipyard U. S. Naval Base Philadelphia 12, Penna.	Commandant U. S. Coast Guard 1300 E Street, N. W. Washington, D. C.	1
	Secretary Ship Structure Committee U. S. Coast Guard Headquarters 1300 E Street, N. W. Washington, D. C.	1

HYDRONAUTICS, Incorporated

-iii-

DISTRIBUTION LIST

Commander Military Sea Transportation Service Department of the Navy Washington 25, D. C.	1	Director Langley Research Center Langley Field, Virginia ATTN: Mr. J. B. Parkinson 2 Mr. I. E. Garrick 1 Mr. D. J. Marten 1
U. S. Maritime Administration GAO Building 441 G Street, N. W. Washington, D. C. ATTN: Division of Ship Design 1 Division of Research 1		Director National Bureau of Standards Washington 25, D. C. ATTN: Fluid Mechanics Div. (Dr. G. B. Schubauer) 1 Dr. G. H. Keulegan 1 Dr. J. M. Franklin 1
Superintendent U. S. Merchant Marine Academy Kings Point, Long Island, New York ATTN: Capt. L. S. McCready (Dept. of Engineering) 1		Armed Services Technical Information Agency Arlington Hall Station Arlington 12, Virginia 10
Commanding Officer and Director U. S. Navy Mine Defense Laboratory Panama City, Florida 1		Office of Technical Services Department of Commerce Washington 25, D. C. 1
Commanding Officer NROTC and Naval Administrative Unit Mass. Inst. of Technology Cambridge 39, Massachusetts 1		California Institute of Technology Pasadena 4, California ATTN: Prof. M. S. Plesset 1 Prof. T. Y. Wu 1 Prof. A. J. Acosta 1
U. S. Army Transportation Research and Development Command Fort Eustis, Virginia ATTN: Marine Transport Division 2		University of California Department of Engineering Los Angeles 24, California ATTN: Dr. A. Powell 1
Director of Research National Aeronautics and Space Administration 1512 H Street, N. W. Washington 25, D. C. 1		Director Scripps Institute of Oceanography University of California La Jolla, California 1
Director Engineering Sciences Div. National Science Foundation 1951 Constitution Avenue, N.W. Washington 25, D. C. 1		Professor M. L. Albertson Department of Civil Engineering Colorado A and M College Fort Collins, Colorado 1

HYDRONAUTICS, Incorporated

-iv-

DISTRIBUTION LIST

Prof. J. E. Cermak Dept. of Civil Engineering Colorado State University Fort Collins, Colorado	Professor J. J. Foody Engineering Department N. Y. State University Maritime College	
Professor W. R. Sears Graduate School of Aeronautical Engr. Cornell University Ithaca, New York	Fort Schulyer, New York	1
State University of Iowa Iowa Inst. of Hydraulic Research Iowa City, Iowa	New York University Inst. of Mathematical Sciences 25 Waverly Place	
ATTN: Dr. H. Rouse Dr. L. Landweber	1 New York 3, New York	
Harvard University Cambridge 38, Massachusetts	ATTN: Prof. J. Keller	1
ATTN: Prof. G. Birkhoff (Dept. of Mathematics)	Prof. J. J. Stoker	1
Prof. G. F. Carrier (Dept. of Mathematics)	Prof. R. Kraichnan	1
Mass. Inst. of Technology Cambridge 39, Massachusetts	1 The Johns Hopkins University	
ATTN: Department of Naval Architecture and Marine Engineering	1 Dept. of Mechanical Engineering Baltimore 18, Maryland	
Prof. A. T. Ippen	ATTN: Prof. S. Corrsin	1
University of Michigan Ann Arbor, Michigan	Prof. O. M. Phillips	2
ATTN: Prof. R. B. Couch (Dept. of Naval Archi- tecture)	1 Mass. Inst. of Technology Dept. of Naval Architecture	
Prof. W. W. Willmarth (Aero. Engrg. Dept.)	1 and Marine Engineering Cambridge 39, Massachusetts	
Prof. M. S. Uberoi (Aero. Engrg. Dept.)	ATTN: Prof. M. A. Abkowitz, Head	
Dr. L. G. Straub, Director St. Anthony Falls Hydraulic Lab. University of Minnesota Minneapolis 14, Minnesota	1 Dr. G. F. Wislicenus	
ATTN: Mr. J. N. Wetzel Prof. B. Silberman	1 Ordnance Research Laboratory	
	1 Pennsylvania State University University Park, Pennsylvania	
	ATTN: Dr. M. Sevik	1
	Professor R. C. DiPrima Department of Mathematics	
	1 Rensselaer Polytechnic Institute Troy, New York	1
	1 Stevens Institute of Technology Davidson Laboratory	
	1 Castle Point Station Hoboken, New Jersey	
	ATTN: Mr. D. Savitsky	1
	Mr. J. P. Breslin	1
	Mr. C. J. Henry	1
	Mr. S. Tsakonas	1

HYDRONAUTICS, Incorporated

-v-

DISTRIBUTION LIST

Webb Institute of Naval Architecture Crescent Beach Road Glen Cove, New York ATTN: Technical Library Director Woods Hole Oceanographic Inst. Woods Hole, Massachusetts Commander Air Research and Development Command Air Force Office of Scientific Research 14th and Constitution Avenue Washington 25, D. C. ATTN: Mechanics Branch	1	Institut für Schiffbau der Universität Hamburg Berliner Tor 21 Hamburg 1, Germany ATTN: Prof. G. P. Weinblum, Director	1
Commander Wright Air Development Division Aircraft Laboratory Wright-Patterson Air Force Base, Ohio ATTN: Mr. W. Mykytow, Dynamics Branch	1	Max-Planck Institut für Strömungsforschung Bottingerstrasse 6/8 Gottingen, Germany ATTN: Dr. H. Reichardt	1
Cornell Aeronautical Laboratory 4455 Genesee Street Buffalo, New York ATTN: Mr. W. Targoff Mr. R. White	1	Hydro-og Aerodynamisk Laboratorium Lyngby, Denmark ATTN: Prof. Carl Prohaska	1
Mass. Inst. of Technology Fluid Dynamics Research Lab. Cambridge 39, Massachusetts ATTN: Prof. H. Ashley Prof. M. Landahl Prof. J. Dugundji	1 1 1	Skipsmodelltanken Trondheim, Norway ATTN: Prof. J. K. Lunde	1
Hamburgische Schiffbau- Versuchsanstalt Bramfelder Strasse 164 Hamburg 33, Germany ATTN: Dr. O. Grim Dr. H. W. Lerbs	1 1	Versuchsanstalt für Wasserbau und Schiffbau Schleuseninsel im Tiergarten Berlin, Germany ATTN: Dr. S. Schuster, Director	1
		Technische Hogeschool Institut voor Toegepaste Wiskunde Julianalaan 132 Delft, Netherlands ATTN: Prof. R. Timman	1
		Bureau D'Analyse et de Techerche Appliquees 2 Rue Joseph Sansboeuf Paris 8, France ATTN: Prof. L. Malavard	1
		Netherlands Ship Model Basin Wageningen, Netherlands ATT: Dr. Ir. J.D. van Manen	1
		Allied Research Assoc., Inc. 43 Leon Street Boston 15, Massachusetts ATTN: Dr. T. R. Goodman	1

HYDRONAUTICS, Incorporated

-vi-

DISTRIBUTION LIST

National Physical Laboratory Teddington, Middlesex, England	Director, Dept. of Mech. Sciences
ATTN: Head Aerodynamics Div. 1 Mr. A. Silverleaf 1	Southwest Research Inst. 8500 Culebra Road San Antonio 6, Texas
Head, Aerodynamics Department Royal Aircraft Establishment Farnborough, Hants, England	ATTN: Dr. H. N. Abramson 1 Mr. G. Ransleben 1 Editor, Applied Mechanics Review 1
ATTN: Mr. M. O. W. Wolfe 2	
Boeing Airplane Company Seattle Division Seattle, Washington ATTN: Mr. M. J. Turner 1	Convair A Division of General Dynamics San Diego, California ATTN: Mr. R. H. Oversmith 1 Mr. A. D. MacLellan 1 Mr. H. T. Brooke 1
Electric Boat Division General Dynamics Corporation Groton, Connecticut ATTN: Mr. Robert McCandliss 1	Dynamic Developments, Inc. 15 Berry Hill Road Oyster Bay, L. I., New York 1
General Applied Sciences Labs, Inc. Merrick and Stewart Avenues Westbury, L.I., New York 1	Dr. S. F. Hoerner 148 Busteed Drive Midland Park, New Jersey 1
Gibbs and Cox, Inc. 21 West Street New York, New York 1	Rand Development Corp. 13600 Deise Avenue Cleveland 10, Ohio ATTN: Dr. A.S. Iberall 1
Grumman Aircraft Engrg. Corp. Bethpage, L.I., New York ATTN: Mr. E. Baird 1 Mr. E. Bower 1	U. S. Rubber Company Research and Development Dept. Wayne, New Jersey ATTN: Mr. L. M. White 1
Grumman Aircraft Engrg. Corp. Dynamic Developments Division Babylon, New York 1	Technical Research Group, Inc. 2 Aerial Way Syosset, L.I., New York ATTN: Mr. Jack Kotik 1
Lockheed Aircraft Corporation Missiles and Space Division Palo Alto, California ATTN: R. W. Kermene 1	Mr. C. Wigley Flat 102 6-9 Charterhouse Square London, E.C. 1, England 1
Midwest Research Institute 425 Volker Blvd. Kansas City 10, Missouri ATTN: Mr. Zeydel 1	AVCO Corp., Lycoming Div. 1701 K St., N.W., Apt. 904 Washington, D. C. ATTN: Mr. T. A. Duncan 1
Mr. J. G. Baker Baker Mfg. Company Evansville, Wisconsin 1	

HYDRONAUTICS, Incorporated

-vii-

DISTRIBUTION LIST

Curtiss-Wright Corp. Research
Division
Turbomachinery Division
Quehanna, Pennsylvania
ATTN: Mr. G. H. Pedersen 1

Hughes Tool Company
Aircraft Division
Culver City, California
ATTN: Mr. M. S. Harned 1

Lockheed Aircraft Corporation
California Division
Hydrodynamics Research
Burbank, California
ATTN: Mr. Kenneth E. Hodge 1

National Research Council
Montreal Road
Ottawa 2, Canada
ATTN: Mr. E. S. Turner 1

The Rand Corporation
1700 Main Street
Santa Monica, California
ATTN: Dr. Blaine Parkin 1

Stanford University
Dept. of Civil Engineering
Stanford, California
ATTN: Dr. Byrne Perry 1
Dr. E. Y. Hsu 1

Waste King Corporation
5550 Harbor Street
Los Angeles 22, California
ATTN: Dr. A. Schneider 1

Chief, Bureau of Naval Weapons
Department of the Navy
Washington 25, D. C.
ATTN: Codes RUAW-4 1
RRRE 1
RAAD 1
RAAD-222 1
DIS-42 1